

Thermochronology of the Talkeetna intraoceanic arc of Alaska: Ar/Ar, U-Th/He, Sm-Nd, and Lu-Hf dating

B. R. Hacker,¹ Peter B. Kelemen,² Matthew Rioux,^{1,3} Michael O. McWilliams,⁴ Philip B. Gans,¹ Peter W. Reiners,⁵ Paul W. Layer,⁶ Ulf Söderlund,⁷ and Jeffrey D. Vervoort⁸

Received 17 September 2010; revised 8 December 2010; accepted 27 December 2010; published 26 February 2011.

[1] As one of two well-exposed intraoceanic arcs, the Talkeetna arc of Alaska affords an opportunity to understand processes deep within arcs. This study reports new Lu-Hf and Sm-Nd garnet ages, ⁴⁰Ar/³⁹Ar hornblende, mica and whole-rock ages, and U-Th/He zircon and apatite ages from the Chugach Mountains, Talkeetna Mountains, and Alaska Peninsula, which, in conjunction with existing geochronology, constrain the thermal history of the arc. Zircon U-Pb ages establish the main period of arc magmatism as 202–181 Ma in the Chugach Mountains and 183–153 Ma in the eastern Talkeetna Mountains and Alaska Peninsula. Approximately 184 Ma Lu-Hf and ~182 Ma Sm-Nd garnet ages indicate that 25–35 km deep sections of the arc remained above ~700°C for as much as 15 Myr. The ⁴⁰Ar/³⁹Ar hornblende ages are chiefly 194–170 Ma in the Chugach Mountains and 175–150 Ma in the Talkeetna Mountains and Alaska Peninsula but differ from zircon U-Pb ages in the same samples by as little as 0 Myr and as much as 33 Myr, documenting a spatially variable thermal history. Mica ages have a broader distribution, from ~180 Ma to 130 Ma, suggesting local cooling and/or reheating. The oldest U-Th/He zircon ages are ~137 to 129 Ma, indicating no Cenozoic regional heating above ~180°C. Although the signal is likely complicated by Cretaceous and Oligocene postarc magmatism, the aggregate thermochronology record indicates that the thermal history

of the Talkeetna arc was spatially variable. One-dimensional finite difference thermal models show that this kind of spatial variability is inherent to intraoceanic arcs with simple construction histories. **Citation:** Hacker, B. R., P. B. Kelemen, M. Rioux, M. O. McWilliams, P. B. Gans, P. W. Reiners, P. W. Layer, U. Söderlund, and J. D. Vervoort (2011), Thermochronology of the Talkeetna intraoceanic arc of Alaska: Ar/Ar, U-Th/He, Sm-Nd, and Lu-Hf dating, *Tectonics*, 30, TC1011, doi:10.1029/2010TC002798.

1. Introduction

[2] There is considerable interest in understanding the processes active in intraoceanic arcs because of the likelihood that such juvenile arcs are the principal sites at which continental crust undergoes initial separation from Earth's mantle. Studies of modern arcs provide insight into how volcanism and deformation evolve temporally and spatially over the lifespan of an arc, but are limited in their ability to decode processes active at depth. Studies of exhumed arc sections provide a complementary view of processes at depth, but many exhumed arcs are too disrupted to preserve a complete crustal section. The Talkeetna arc is one of two intraoceanic arcs on Earth where the entire section from the upper mantle tectonite at the base of the arc through the sediments capping the volcanic carapace is well exposed [Burns, 1985; DeBari and Coleman, 1989]; the second is the Kohistan arc [Jan and Howie, 1981]. As such, it provides an important focus site where arc processes can be studied at a range of paleodepths. U-Pb zircon chronology shows that the main axis of the Talkeetna arc in the Chugach Mountains was active from 202 Ma to 181 Ma [Rioux *et al.*, 2007], and was accreted to North America by the Late Jurassic or Early Cretaceous [Burns, 1985; Plafker *et al.*, 1989]. This study characterizes and interprets the thermal history of the Talkeetna arc to understand the thermal history of an active intraoceanic magmatic arc at depth. This objective is accomplished by summarizing the available radiochronology and fossil ages and reporting new ⁴⁰Ar/³⁹Ar hornblende, mica, and whole-rock ages, Lu-Hf garnet ages, Sm-Nd garnet ages, and zircon and apatite U-Th/He ages. These ages are then interpreted with the aid of a simple model for the Talkeetna arc.

2. Geologic Setting of the Talkeetna Arc

[3] The Talkeetna arc consists of a series of volcanic and plutonic bodies that crop out from the Chugach Mountains

¹Department of Earth Science, University of California, Santa Barbara, California, USA.

²Lamont-Doherty Earth Observatory, Earth Institute at Columbia University, Palisades, New York, USA.

³Now at Department of Earth, Atmospheric, and Planetary Sciences, Massachusetts Institute of Technology, Cambridge, Massachusetts, USA.

⁴Earth Science and Resource Engineering, Commonwealth Scientific and Industrial Research Organisation, Pullenvale, Queensland, Australia.

⁵Department of Geosciences, University of Arizona, Tucson, Arizona, USA.

⁶Geophysical Institute and Department of Geology and Geophysics, University of Alaska Fairbanks, Fairbanks, Alaska, USA.

⁷Department of Earth and Ecosystem Sciences, Lund University, Lund, Sweden.

⁸School of Earth and Environmental Sciences, Washington State University, Pullman, Washington, USA.

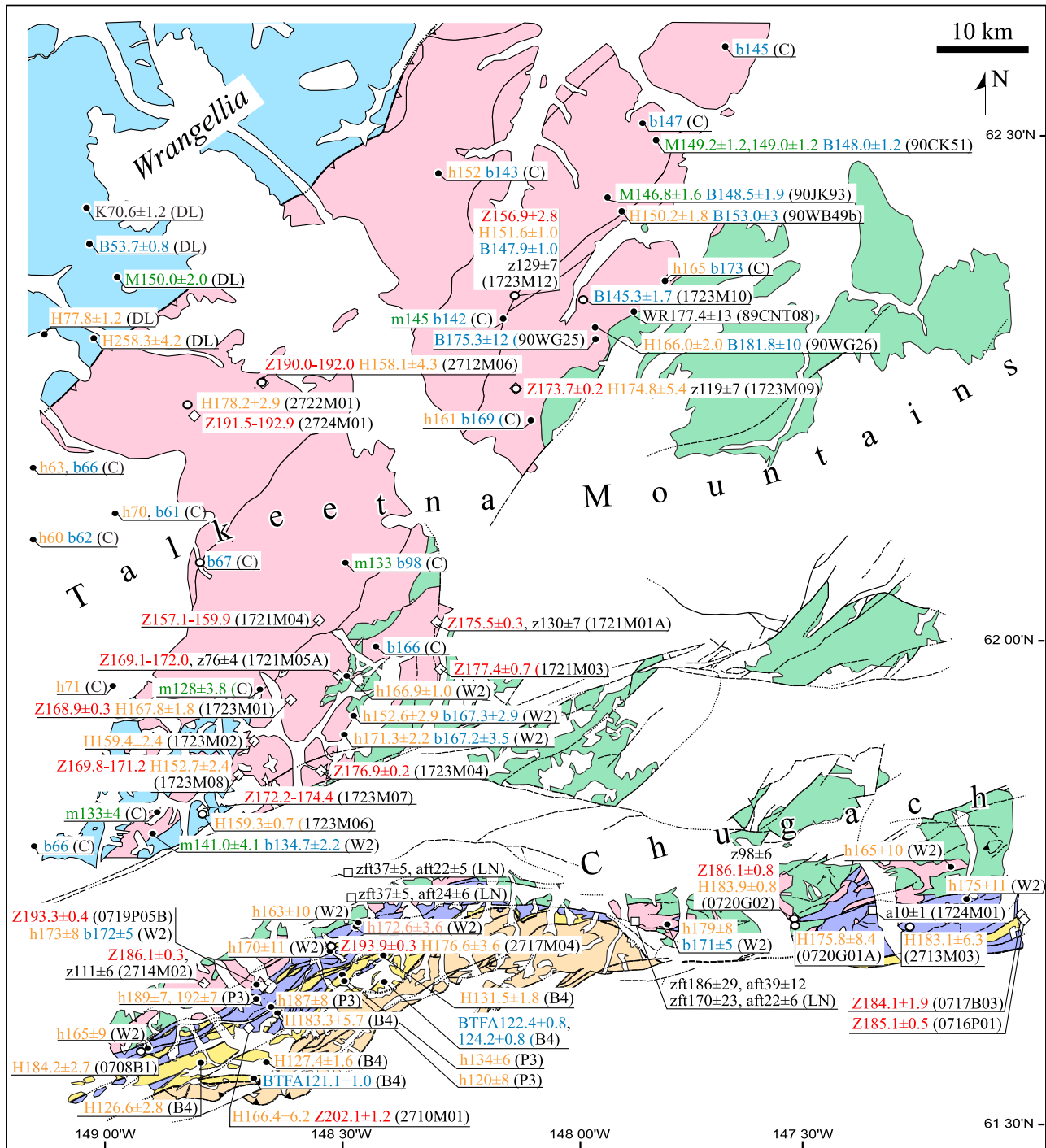


Figure 1. Geochronology of the Talkeetna and Chugach mountains. All uncertainties are 2σ except for those from *Csejtey et al.* [1978], which are unknown; uncertainties include uncertainty in standard ages and decay constants. Questionable ages are shown in italics. Ages are from this study except for the following: B4, *Barnett et al.* [1994]; DL, *Drake and Layer* [2001]; C, *Csejtey et al.* [1978]; LN, *Little and Naeser* [1989]; O9, *Onstott et al.* [1989]; P3, *Pavlis* [1983]; P9, *Plafker et al.* [1989]; SO, *Sisson and Onstott* [1986]; W1, *Winkler et al.* [1981]; W2, *Winkler* [1992]. Thick lines are faults, and thin lines are depositional and intrusive contacts. Inset map base from Google maps (Google Earth imagery © 2010 Google Inc. Used with permission).

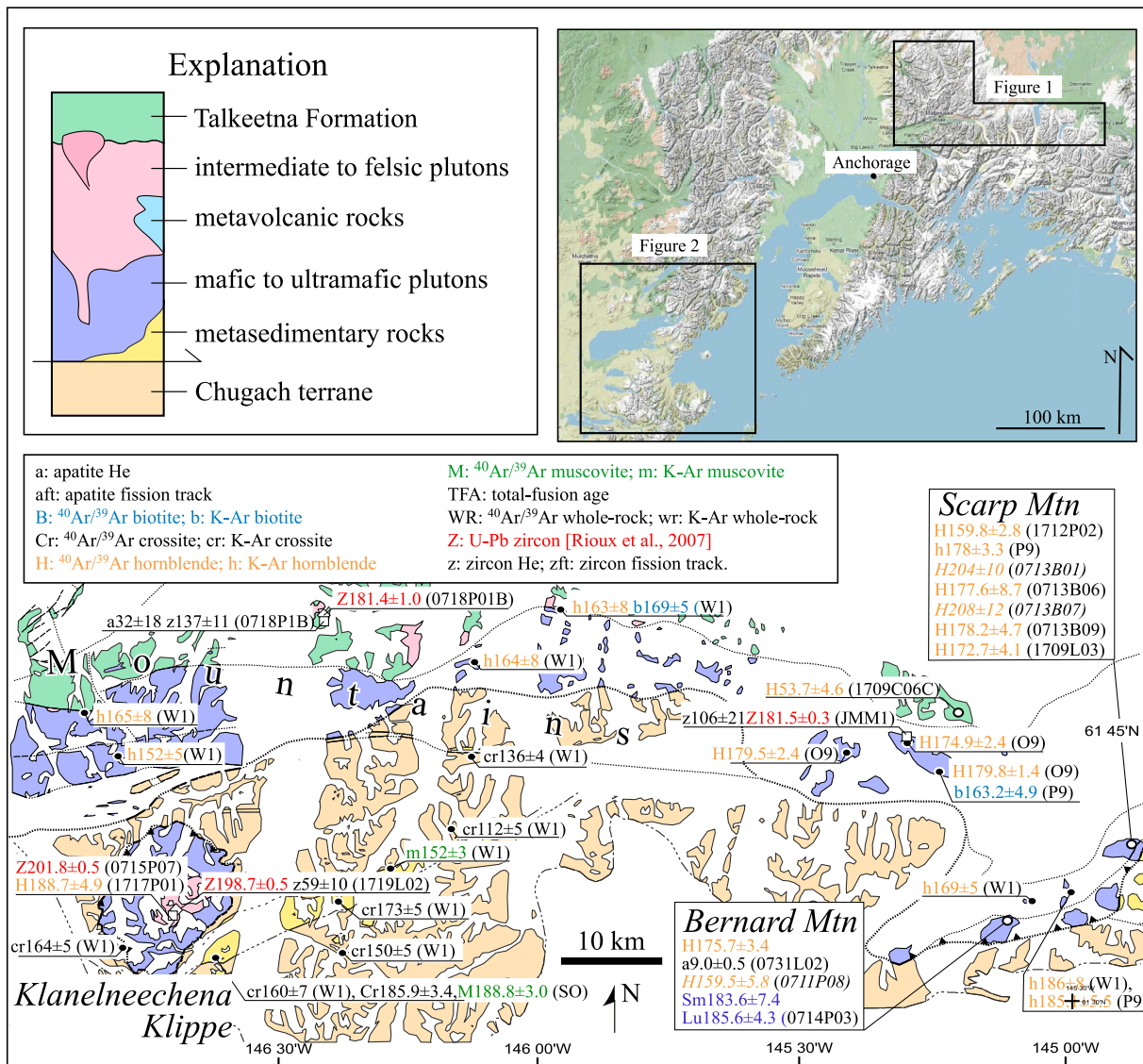


Figure 1. (continued)

in the east to the Alaska Peninsula and Kodiak archipelago in the southwest (Figures 1 and 2). Exposures in the Chugach and Talkeetna mountains (Figure 1) include all the types of rocks that comprise a magmatic arc, volcanoclastic rocks (the Talkeetna Formation), hypabyssal and plutonic rocks, and mantle peridotite [Burns, 1985; DeBari and Coleman, 1989; Plafker et al., 1989; Kelemen et al., 2003b; Mehl et al., 2003; Clift et al., 2005; Greene et al., 2006; Rioux et al., 2010]. Using the thickness of the coeval volcanic section [Clift et al., 2005] and thermobarometry on igneous and metamorphic rocks at various levels within the arc, Hacker et al. [2008] reconstructed the pseudostratigraphy of the arc as: 5 km of volcanic rocks, 4–14 km of felsic plutons, 9–16 km of mafic plutons, and 4–10 km of basal garnet gabbro-norite.

[4] The Talkeetna arc intrudes the Wrangellia terrane to the north [Rioux et al., 2007], and is bounded to the south by the Border Ranges fault system, which is interpreted as a heavily modified subduction thrust [Roeske et al., 2003; Pavlis and Roeske, 2007]. Beneath the Border Ranges fault system lie Late Triassic blueschist, Cretaceous mélange and turbidites of the Chugach terrane [Plafker et al., 1994]. A klippe of arc plutonic rocks south of the Border Ranges fault zone in the Klanelneechena area [Winkler et al., 1981] has been correlated with the Talkeetna arc. The Talkeetna arc is overlain by a sequence of Jurassic to Oligocene sedimentary and volcanic rocks and intruded by a variety of Late Cretaceous to Oligocene rocks reflecting Jurassic through Recent plate convergence [Plafker et al., 1994; Trop and Ridgeway, 2007].

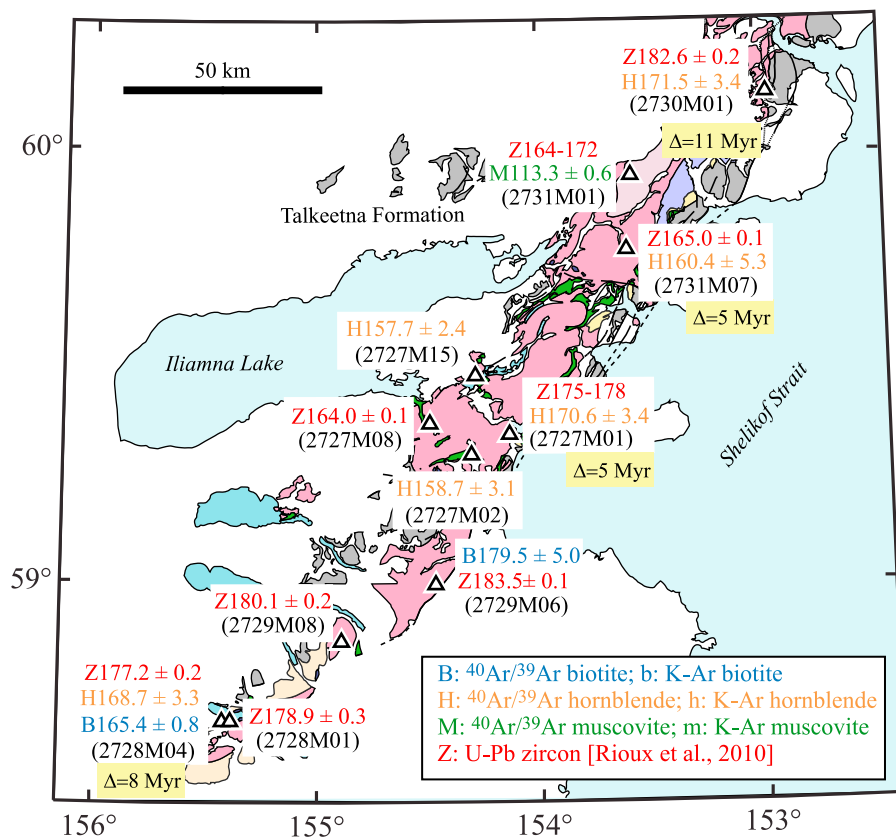


Figure 2. Geochronology of the Talkeetna arc along the Alaska Peninsula. U-Pb zircon ages are from *Rioux et al.* [2010]; other data are from this study. See Figure 1 for explanation of symbols and colors. Yellow boxes show differences in zircon U-Pb and hornblende ages.

[5] This study builds on an existing geochronology data set that is examined in detail later in the paper. The first, quite extensive, studies of the Talkeetna and Chugach mountains, by *Csejtey et al.* [1978] and *Winkler et al.* [1981] reported dozens of hornblende and mica K/Ar ages, revealing that the Talkeetna arc cooled in the Jurassic and that there was significant Tertiary magmatism in the Talkeetna Mountains. Later K/Ar and $^{40}\text{Ar}/^{39}\text{Ar}$ dating by *Pavlis* [1983], *Plafker et al.* [1989], *Onstott et al.* [1989], *Winkler* [1992], and *Barnett et al.* [1994] reinforced this data set and revealed an additional significant Late Cretaceous pulse of magmatism in the western Chugach Mountains. *Little and Naeser* [1989] used fission track dating of apatite and zircon to show that some portions of the Talkeetna arc might have cooled to $<350^\circ\text{C}$ during the Jurassic, and that widespread felsic stocks in the Chugach Mountains were Oligocene. The most recent $^{40}\text{Ar}/^{39}\text{Ar}$ study, by *Drake and Layer* [2001], reported eleven Jurassic to Cretaceous cooling ages from the northern Talkeetna Mountains. The intrusive history of the Talkeetna arc has been illuminated in some detail by the chemical abrasion U-Pb TIMS work of *Rioux et al.* [2007, 2010]. To these data sets, we add Sm-Nd and Lu-Hf dating of garnets from the base of the arc, $^{40}\text{Ar}/^{39}\text{Ar}$ hornblende and mica ages from all levels of the arc plutonic section, and

U-Th/He ages of the arc plutonic section (Table 1 and auxiliary material).¹

3. Analytical Techniques

[6] Sm-Nd and Lu-Hf dating was completed on two samples (Table 2 and Figure 3) at the University of Arizona using an Isoprobe MC-ICP-MS. For analytical details, see *Patchett et al.* [2004]. We used the ^{176}Lu decay constant of $1.867 \pm 0.008 \text{ E-11/yr}$ from *Söderlund et al.* [2004]; and the ^{147}Sm decay constant of $6.54 \pm 0.05 \text{ E-12/yr}$ from *Lugmair and Marti* [1978].

[7] Argon isotopic ratios from hornblende, muscovite, biotite, and whole rocks were measured using MAP 216 mass spectrometers at Stanford University, UCSB, and the University of Alaska; for analytical details, see *Hacker and Wang* [1995], *Calvert et al.* [1999], and *Newberry et al.* [1998], respectively. Ages are based on an age of $28.619 \pm 0.068 \text{ Ma}$ (total uncertainty, including uncertainty in decay constant) for the Taylor Creek sanidine irradiation fluence monitor [*Renne et al.*, 2010] and an age of $527.6 \pm 0.4 \text{ Ma}$ for MMhb-1 (P. Renne, personal communication, 2010). We

¹Auxiliary materials are available at <ftp://ftp.agu.org/apend/tc/2010tc002798>.

Table 1. Sample List

Sample	UTM N	UTM E	Rock Type	Methods
0708B01	379615	6817806	amphibolite	40/39
0711P08	599692	6829302	garnet gabbro	40/39
0712P08	612086	6835495	garnet gabbro	Lu-Hf and Sm-Nd
0713B01	611879	6835507	gabbro	40/39
0713B06	611426	6835402	tonalite	40/39
0713B07	611159	6835499	gabbro	40/39
0713B09	610531	6835090	hornblendite	40/39
0714P04	599966	6829377	garnet gabbro	Lu-Hf and Sm-Nd
0714P07b	599966	6829377	garnet gabbro	40/39
0718P01B	468823	6860932	gabbro	U-Th/He
0720G01a	530461	6843438	diorite	40/39
0720G02	469477	6843396	quartz diorite	40/39
0731L02	599421	6868438	garnet gabbro	40/39
1709C06c	591140	6849946	volcanic rock	40/39
1709L03	610865	6835510	garnet gabbro	40/39
1712P02	512027	6834772	hornblendite	40/39
1717P01	514509	6830991	hornblendite	40/39
1719L02	514744	6831007	garnet pyroxenite	U-Th/He
1721M01	430974	6876836	granodiorite	U-Th/He
1721M05	419863	6871256	quartz diorite	U-Th/He
1723M01	414618	6868471	quartz diorite	40/39
1723M02	411233	6864264	quartz diorite	40/39
1723M06	405233	6856125	amphibolite	40/39
1723M08	408019	6860756	quartz diorite	40/39
1723M09	440158	6902343	granodiorite	40/39, U-Th/He
1723M10	447622	6915897	trondhjemite	40/39
1723M12	440230	6916915	trondhjemite	40/39, U-Th/He
2710M01	411145	6833735	gabbro	40/39
2712M06	411553	6903246	pegmatite	40/39
2714M02	404764	6836991	tonalite	U-Th/He
2713M03	483274	6843023	gabbro	40/39
2717M04	418800	6841169	gabbro	40/39
2722M01	402870	6901919	gabbro	40/39
2727M02	575233	6573754	tonalite	40/39
2727M15	427268	6593726	quartz diorite	40/39
2728M04	362039	6507187	tonalite	40/39
2729M06	416543	6541058	tonalite	40/39
2730M01	502499	6666424	diorite	40/39
2731M01	466290	6644241	trondhjemite	40/39
2731M07	465440	6627797	quartz diorite	40/39
89CNT08	453921	6910535	volcanic rock	40/39
90JK93	450452	6924322	trondhjemite	40/39
90KC51	455587	6929851	trondhjemite	40/39
90WG25	449386	6908769	granite	40/39
90WG26	449264	6909297	tonalite	40/39
90WG49B	453166	6921559	gneiss	40/39
JMM1	589390	6846813	pegmatite	U-Th/He

used the ^{40}K decay constant of $5.5492 \pm 0.0186 \text{ E-}10/\text{yr}$ from *Renne et al.* [2010]. All previously reported K-Ar and $^{40}\text{Ar}/^{39}\text{Ar}$ ages from the study area were updated to reflect these new constants.

[8] U-Th/He ages of zircon and apatite were measured at Yale University on single-grain aliquots using standard procedures involving laser heating and cryogenically processed He analysis on a gas source mass spectrometer, followed by HR-ICP-MS measurement of parent nuclides, as described in the work by *Reiners et al.* [2004] and *Reiners* [2005].

[9] The reported and discussed data included geochronologic analyses using several different decay schemes and collected at several different laboratories; this approach is necessary to understand both the thermal and temporal history of the arc crust. When comparing the data, however, it is important to account for interlaboratory biases and intertechnique biases. Important systematic uncertainties in the U-Pb zircon data include uncertainties in the U-Pb tracer calibration and U-Pb decay constants. *Rioux et al.* [2007] reported tracer uncertainties for the U-Pb analyses of 0.1–0.2% (2σ) based on interlaboratory comparisons of the Temora and R33 zircon standards as part of the EARTHTIME initiative. Counting statistics during the measurement of the U half-lives lead to minimum 2σ decay constant uncertainties for ^{238}U of $\pm 0.107\%$ [*Jaffey et al.*, 1971; *Mattinson*, 1987]. All U-Pb zircon ages discussed herein are $^{206}\text{Pb}/^{238}\text{U}$ ages and include the tracer and decay-constant uncertainties. Many previous studies have noted systematic offsets between U-Pb and $^{40}\text{Ar}/^{39}\text{Ar}$ ages [e.g., *Schoene et al.*, 2006], most likely related to uncertainties in the ^{40}K decay constants and/or the $^{40}\text{Ar}^*/^{40}\text{K}$ of common standards. In this study, we used the decay constant and Taylor Creek sanidine age of *Renne et al.* [2010]. The ^{176}Lu decay constant of *Söderlund et al.* [2004] is calibrated against U-Pb data from terrestrial samples. Finally, the ^{147}Sm decay constant from *Lugmair and Marti* [1978] represents an average of four direct counting experiments, and is consistent with the U decay constants of *Jaffey et al.* [1971]. Note that the age offsets discussed in this manuscript are generally large compared to potential interlaboratory biases and decay constant uncertainties.

[10] Age uncertainties reported in this paper are 2σ or 95% confidence interval total uncertainties (i.e., including

Table 2. Lu-Hf and Sm-Nd Data^a

Sample	Weight (g)	$^{147}\text{Sm}/^{144}\text{Nd}$	$^{143}\text{Nd}/^{144}\text{Nd}$	$\pm 2\sigma$	Sm (ppm)	Nd (ppm)	Epsilon Nd (0)	$\pm 2\sigma$	$^{176}\text{Lu}/^{177}\text{Hf}$	$^{176}\text{Hf}/^{177}\text{Hf}$	$\pm 2\sigma$	Lu (ppm)	Hf (ppm)	Epsilon Hf (0)	$\pm 2\sigma$
0712P08															
cpx	0.08835	0.279999	0.513075	10	1.34	2.893	8.5	0.2	0.024756	0.283069	18	0.3233	1.853	10.0	0.6
whole rock	0.18093	0.329457	0.513139	12	0.704	1.293	9.8	0.2	0.277613	0.284059	33	0.3449	0.1763	45.1	1.2
garnet	0.0885	1.015639	0.513944	31	0.456	0.271	25.5	0.6	2.004308	0.290025	103	0.9252	0.0656	256.0	3.6
0714P03															
cpx	0.1437	0.292261	0.513112	11	0.911	1.88	9.2	0.2	0.059879	0.284243	22	0.0812	0.1924	51.6	0.8
whole rock	0.18879	0.31971	0.513141	10	0.971	1.836	9.8	0.2	0.145014	0.283543	21	0.1941	0.1899	26.8	0.7
garnet	0.09804	0.994781	0.513954	29	0.674	0.41	25.7	0.6	1.141705	0.286996	78	0.7037	0.0875	148.9	2.8

^aUncertainties on $^{143}\text{Nd}/^{144}\text{Nd}$ and $^{176}\text{Hf}/^{177}\text{Hf}$ ratios are in-run errors calculated as the standard error of the mean. For Sm-Nd and Lu-Hf ages, we used the following uncertainties, based on either reproducibility of the standards (calculated as 2 sigma standard deviations) or the in-run error, whichever was larger. Uncertainty on $^{147}\text{Sm}/^{144}\text{Nd}$ is 0.2%. Uncertainty on $^{143}\text{Nd}/^{144}\text{Nd}$ is 0.005% or in-run uncertainty, whichever is greater. Uncertainty on $^{176}\text{Lu}/^{177}\text{Hf}$ is 0.5%. Uncertainty on $^{176}\text{Hf}/^{177}\text{Hf}$ is 0.01% or in-run uncertainty, whichever is greater.

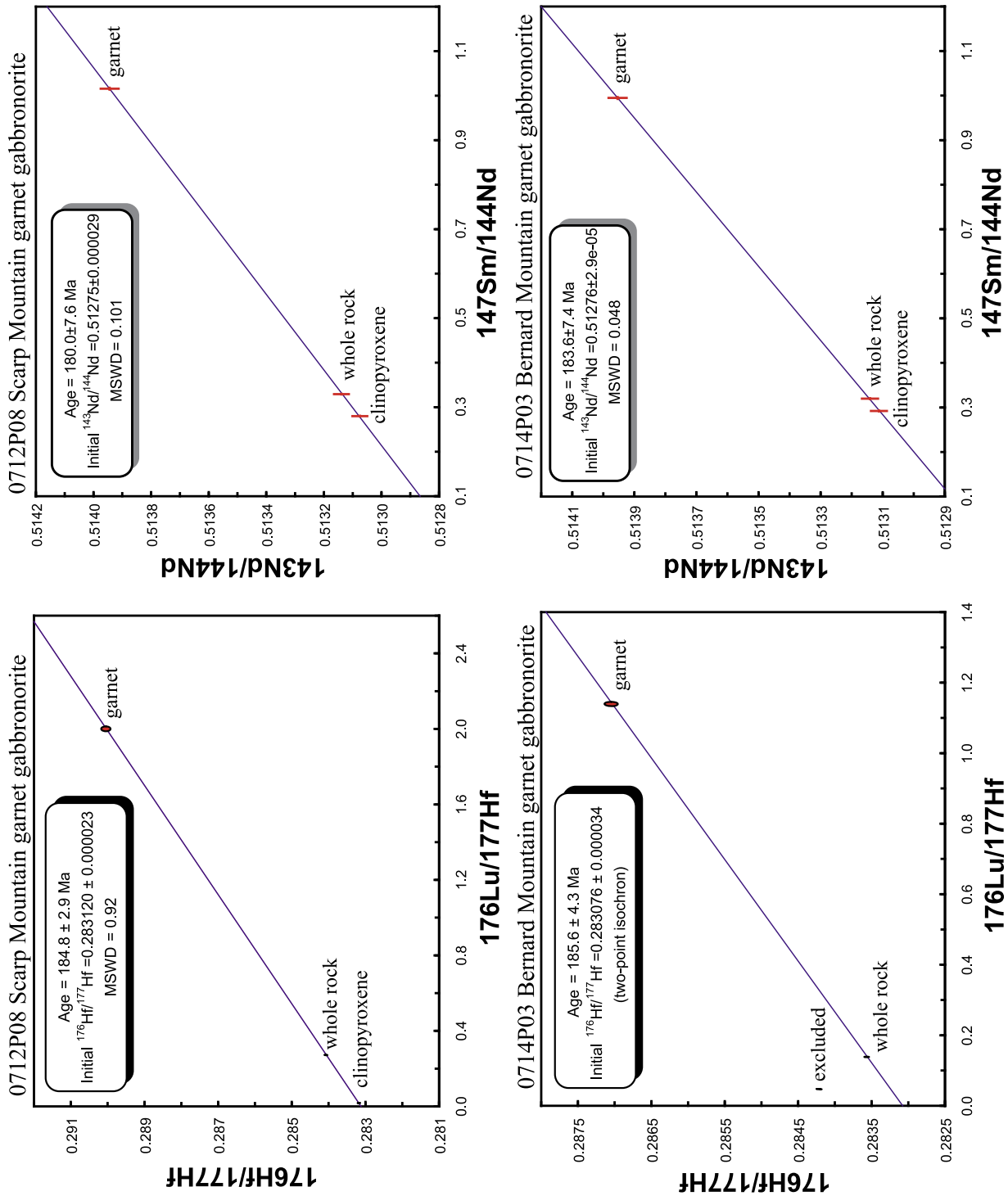


Figure 3. New Lu-Hf and Sm-Nd analyses for the Talkeetna arc. The 2σ uncertainties are shown. Calculations and figures produced with *Isoplot* [Ludwig, 2003].

internal errors, such as counting statistics, and external errors, such as uncertainties in decay constants).

4. Closure Temperatures

[11] U-Pb zircon ages reported in this paper are presumed to be crystallization ages, as discussed by *Rioux et al.* [2007, 2010]. The $^{40}\text{Ar}/^{39}\text{Ar}$ ages are presumed to be cooling ages because all of the dates reported in this paper are from plutonic rocks with high crystallization temperatures; two exceptions to this are the (sub)volcanic rocks 1709C06c and 89CNT08, for which the hornblende ages likely approximate the crystallization age. The hornblende, muscovite, and biotite samples cooled at rates of ~ 10 K/Myr (see below) and have grain sizes of 100–500 microns, implying closure temperatures of $\sim 510^\circ\text{C}$ – 575°C , 425°C – 475°C , and 300°C – 350°C , respectively, based on the work by *Harrison* [1981], *Harrison et al.* [2009], *Kirschner et al.* [1996], *Grove and Harrison* [1996] and *Dunlap* [2000]. The Sm-Nd and Lu-Hf ages reported are also cooling ages because these systems probably closed at temperatures of 700°C – 750°C [*Ganguly and Tirone*, 1999; *Scherer et al.*, 2000; *Van Orman et al.*, 2002; *Kylander-Clark et al.*, 2007, 2009], below the peak temperatures of 800°C – 1000°C [*Hacker et al.*, 2008]. We assume closure temperatures of 340°C for fission tracks in zircon, 180°C for He in zircon [*Reiners and Brandon*, 2006], and 62°C for He in apatite [*Flowers et al.*, 2009]. Note that $^{40}\text{Ar}/^{39}\text{Ar}$ biotite and zircon U-Th/He ages from nearby samples within the arc are not equivalent (see below), implying inaccuracies in these assumed closure temperatures.

[12] We used ages and closure temperatures to reconstruct cooling histories for the Talkeetna arc, but this effort was hampered by two main issues: (1) only a subset of samples contained both zircon and hornblende, inhibiting the reconstruction of the high-temperature histories of individual samples, and (2) K-feldspars in the Chugach Mountains show pervasive hydrothermal alteration, prohibiting meaningful $^{40}\text{Ar}/^{39}\text{Ar}$ analysis.

5. Sm-Nd and Lu-Hf Ages

[13] Two garnet gabbro samples, 0712P08 from the Klanelneehena Klippe and 0714P03 from Bernard Mountain, gave well-constrained isochrons using data collected at the University of Arizona. The Klanelneehena Klippe sample yielded a Sm-Nd age of 180.0 ± 7.6 Ma (2σ ; MSWD = 0.1) and a Lu-Hf age of 184.8 ± 2.9 Ma (MSWD = 0.9); the Bernard Mountain sample gave indistinguishable ages of 183.6 ± 7.4 Ma (MSWD = 0.05) and 185.6 ± 4.3 Ma (two-point isochron). The garnets in the Klanelneehena Klippe are magmatic and record PT conditions of $\sim 800^\circ\text{C}$ and 0.7 GPa, whereas the Bernard Mountain garnets are metamorphic and record $\sim 930^\circ\text{C}$ and 1 GPa [*Hacker et al.*, 2008].

6. The $^{40}\text{Ar}/^{39}\text{Ar}$ Ages

[14] $^{40}\text{Ar}/^{39}\text{Ar}$ dating focused on hornblende to reconstruct the high-temperature cooling history of the arc, but muscovite, biotite and whole-rock samples were also measured (Table 3 and Figure 4). To assess the age of each sample, we considered only the steps with K/Ca ratios

appropriate for the sample; for a few samples this meant that some low-temperature steps were discarded. Unfortunately, the rather low K_2O contents of the hornblendes and the one whole-rock sample produced age spectra of less-than-optimal precision. A minority of the samples (0720G01a, 0720G02, 0731L02, 1709C06c, 1717P01, 1723M01, 1723M08, 1723M09 bio, 2712M06, 2713M03, 2727M01, 2727M02, 2731M07, 90JK93, 90JK93, 90KC51, 90KC51, 90KC51, 90WG25, 90WG26 hornblende, and 90WG49B hornblende) yielded release spectra with plateaus and inverse isochron $^{40}\text{Ar}/^{36}\text{Ar}$ intercepts equivalent to the atmosphere (295.5); for these samples we accept the plateau age as the best age for the sample. Four samples (0713B07, 0713B09, 0714P07b, and 89CNT08) gave isochrons with $^{40}\text{Ar}/^{36}\text{Ar}$ intercepts equivalent to atmosphere, but for so few steps that we prefer the isochron ages with their higher uncertainties to the more precise weighted mean age derived from the step ages. A modest subset of the samples (0711P08, 0713B01, 0713B06, 1709L03, 1712P02, 2722M01, and 2728M04) gave isochrons with $^{40}\text{Ar}/^{36}\text{Ar}$ intercepts greater than 295.5, indicative of excess ^{40}Ar ; for these samples we use the isochron age as the best age of the sample. Another subset of samples (0708B01, 1723M02, 1723M10, 1723M12, 2710M01, 2717M04, 2727M15, 2729M06, 2730M01b, 2731M01, 1723M12) gave $^{40}\text{Ar}/^{36}\text{Ar}$ intercepts less than atmospheric, generally indicative of either low signal:blank ratios, clustered isotopic ratios (i.e., insufficient spread in $^{40}\text{Ar}/^{36}\text{Ar}$ or $^{40}\text{Ar}/^{39}\text{Ar}$), or very high radiogenic yields (low $^{40}\text{Ar}/^{36}\text{Ar}$ ratios). For these samples the isochrons are poorly defined, but the spectra well behaved, so we accept the plateau age of the sample as the best age. Biotites 90WG49B and 90WG26 have K_2O contents less than 5 wt % and ages older than hornblende from the same sample. These low K_2O contents likely reflect alteration, such that the hornblende ages most likely better reflecting the cooling age of these samples.

7. U-Th/He Ages

[15] U-Th/He ages were measured for zircon from ten samples and for apatite from three (Table 4). Two or three single-grain aliquots were measured from each and a weighted mean age (uncertainty at 95% C.I.) was calculated for each sample. The zircon He ages range from 130 Ma to 59 Ma, with the oldest ~ 20 Myr younger than nearby zircon crystallization ages. The apatite ages are considerably younger, with the two well-behaved samples giving ages of ~ 9 Ma. Two aliquots from a third sample yielded apatite He ages of 26 and 38 Ma; these latter ages are correlated with equivalent uranium ($\text{U}+0.235\text{Th}$), consistent with an explanation involving radiation damage effects [*Flowers et al.*, 2009] on diffusivity in a slowly cooled or reheated sample.

8. Interpretation

8.1. Chugach Mountains

[16] The Chugach and Talkeetna mountains now have a relatively robust geochronology database that shows spatial patterns, including cooling histories (Figures 1, 5, and 6). The zircon U-Pb ages from the Chugach Mountains are

Table 3. The $^{40}\text{Ar}/^{39}\text{Ar}$ Summary Data^a

Sample	Min.	Loc.	Mass (mg)	wt % K ₂ O	WMPA	(2σ)	IA	(2σ)	$^{40}\text{Ar}/^{36}\text{Ar}$ (2σ)	MSWD
0708B01	hbl	UCSB	9.7		<i>184.2</i>	2.7	186.2	2.8	225 ± 50	1.7
0711P08	hbl	UCSB	11.5	0.10	na		<i>159.5</i>	5.8	402 ± 8	0.6
0713B01	hbl	UCSB	8.5		na		<i>203.9</i>	10	353 ± 15	1.6
0713B06	hbl	UCSB	10.5	0.25	na		<i>177.6</i>	8.7	606 ± 32	1.5
0713B07	hbl	UCSB	13.8	0.20	na		<i>208</i>	12	304 ± 35	0.0
0713B09	hbl	UCSB	11.0		na		<i>178.2</i>	4.7	299 ± 17	1.4
0714P07b	hbl	UCSB	10.8		na		357.4	33	281 ± 20	1.8
0720G01a	hbl	SU	11.8		<i>177.5</i>	8.4	180.4	6.7	291 ± 52	0.2
0720G02	hbl	UCSB	12.3	0.25	<i>183.9</i>	0.8	183.3	1.1	284 ± 15	1.6
0731L02	hbl	SU	12.7		181.7	6.3	<i>175.7</i>	3.4	326 ± 32	1.8
1709C06c	hbl	SU	12.6		<i>53.7</i>	4.6	51.3	3.3	314 ± 54	0.8
1709L03	hbl	SU	12.5	0.22	182.7	6	<i>172.7</i>	4.1	350 ± 20	1.3
1712P02	hbl	SU	20.6		163.6	9.6	<i>159.8</i>	2.8	323 ± 12	1.2
1717P01	hbl	SU	24.9	0.30	<i>188.7</i>	4.9	189.8	1.4	280 ± 12	0.7
1723M01	hbl	SU	7.7	1.00	<i>167.8</i>	1.8	166.3	2.6	377 ± 240	2.3
1723M02	hbl	SU	8.7		<i>159.4</i>	2.4	161.0	1.1	233 ± 28	1.6
1723M06	hbl	UCSB	9.8		<i>159.3</i>	0.7	161.5	2.2	247 ± 40	0.8
1723M08	hbl	SU	11.0	0.50	<i>152.7</i>	2.4	151.2	2.4	320 ± 34	1.4
1723M09	hbl	SU	7.6	0.55	<i>174.8</i>	5.4	175.3	3.5	271 ± 54	0.5
1723M10	bio	SU	0.5		<i>145.3</i>	1.7	147.6	1.8	94 ± 58	1.2
1723M12	bio	SU	1.4		<i>147.9</i>	1.0	138.1	5.9	2350 ± 5000	1.0
1723M12	hbl	SU	8.4	1.8	<i>151.6</i>	1.0	142.9	4.2	1024 ± 290	0.5
2710M01	hbl	SU	6.8		<i>166.4</i>	6.2	183.1	6.6	78 ± 200	1.9
2712M06	hbl	SU	7.6	0.60	<i>158.1</i>	4.3	157.1	11	367 ± 90	0.1
2713M03	hbl	SU	5.6	0.35	<i>183.1</i>	6.3	182.3	2	320 ± 26	1.5
2717M04	hbl	SU	12.0	0.50	<i>176.6</i>	3.6	180.9	5.4	159 ± 96	1.7
2722M01	hbl	SU	20.1	0.25	<i>178.2</i>	2.9	173.9	3.7	402 ± 84	2.1
2727M01	hbl	SU	1.8	0.45	<i>170.6</i>	3.4	168.5	9.4	399 ± 210	0.7
2727M02	hbl	SU	17.7	0.25	<i>158.7</i>	3.1	162.3	1.4	244 ± 16	1.2
2727M15	hbl	SU	16.6	0.50	<i>157.7</i>	2.4	153.3	2.2	424 ± 64	1.3
2728M04	hbl	SU	5.8	0.65	<i>168.7</i>	3.3	165.4	4.4	457 ± 168	1.2
2728M04	bio	SU	3.2		<i>165.4</i>	0.8	164.1	0.8	509 ± 96	1.7
2729M06	bio	SU	22.5		none		<i>179.5</i>	5	2582 ± 680	1.4
2730M01	hbl	SU	2.5	0.30	<i>171.5</i>	3.4	179	1.6	109 ± 18	2.2
2731M01	mus	SU	1.8		<i>113.4</i>	0.6	114.1	0.5	225 ± 40	1.9
2731M07	hbl	SU	13.7	0.30	<i>160.4</i>	5.3	151.1	13	510 ± 120	0.7
89CNT08	wr	UAF	249	0.82	174.0	6.7	<i>176.8</i>	13	294 ± 230	12
90JK93	mus	UAF	17.4	10.0	<i>146.8</i>	1.6	145.7	3.4	396 ± 264	0.5
90JK93	bio	UAF	48.9	9.3	<i>148.5</i>	1.9	146.8	2.4	502 ± 198	0.8
90KC51	bio	UAF	53.4	7.9	<i>148.0</i>	1.2	148.6	2	281 ± 40	0.3
90KC51	mus	UAF	54.5	11.0	<i>149.2</i>	1.2	148.7	1.4	318 ± 62	0.3
90KC51	mus 250–300 micron	UAF	47.7	10.0	<i>149.0</i>	1.2	147.2	1.8	374 ± 62	0.5
90WG25	bio	UAF	63.9	5.9	na	1.5	<i>175.3</i>	12	468 ± 743	27
90WG26	hbl	UAF	315	0.44	<i>166.0</i>	2.0	166.3	3.6	293 ± 26	1.1
90WG26	bio	UAF	50.5	4.7	na	10	<i>181.8</i>	9.7	290 ± 304	73
90WG49B	hbl	UAF	335	0.75	<i>150.2</i>	1.8	145	1.6	302 ± 13	0.6
90WG49B	bio	UAF	75.2	3.8	<i>153.0</i>	3.0	149.2	3.5	561 ± 238	1.5

^aMin., mineral; bio, biotite; hbl, hornblende; mus, K-white mica; loc., analysis location; SU, Stanford University; UAF, University of Alaska, Fairbanks; UCSB, University of California, Santa Barbara; J, irradiation parameter; K₂O determined by electron microprobe (SU, UCSB) or mass spectrometry (UAF); WMPA, weighted mean plateau age (Ma); IA, isochron age (Ma); MSWD, mean of squared weighted deviates for isochron; $^{40}\text{Ar}/^{36}\text{Ar}$, trapped $^{40}\text{Ar}/^{36}\text{Ar}$ ratio of isochron; 2σ includes uncertainty in decay constant and monitor age; na, not applicable; italic text indicates preferred age (see text).

exclusively from felsic to intermediate rocks, and range from 202 to 181 Ma, or 20 Myr [Rioux *et al.*, 2007]; zircons from the volumetrically dominant mafic suite remain undated. This range is similar to the age of the volcanic Talkeetna Formation which is as old as 207 Ma (on the Alaska Peninsula [Amato *et al.*, 2007]) and is unconformably overlain by the early Bajocian (172–168 Ma [Gradstein *et al.*, 2004]) Tuxedni Formation [Imlay, 1984].

[17] Although the two samples dated by the Lu-Hf and Sm-Nd methods come from different depths within the Talkeetna arc, and garnet is metamorphic in one sample and

igneous in the other, they both give Lu-Hf ages of ~185 Ma and Sm-Nd ages of ~182 Ma. The igneous garnet from the Klanelneechena klippe (1712P08), inferred to have formed at ~800°C and 0.7 GPa [Hacker *et al.*, 2008], is ~15 Myr younger than nearby zircon U-Pb ages, suggesting a prolonged residence time at temperatures >700°C; hornblende from a sample <250 m away is equivalent in age. The metamorphic garnet from base of the arc in the Bernard Mountain area, formed at ~930°C and 1.0 GPa [Hacker *et al.*, 2008], is only a few million years older than hornblende from an outcrop 1.6 km away (0731L02).

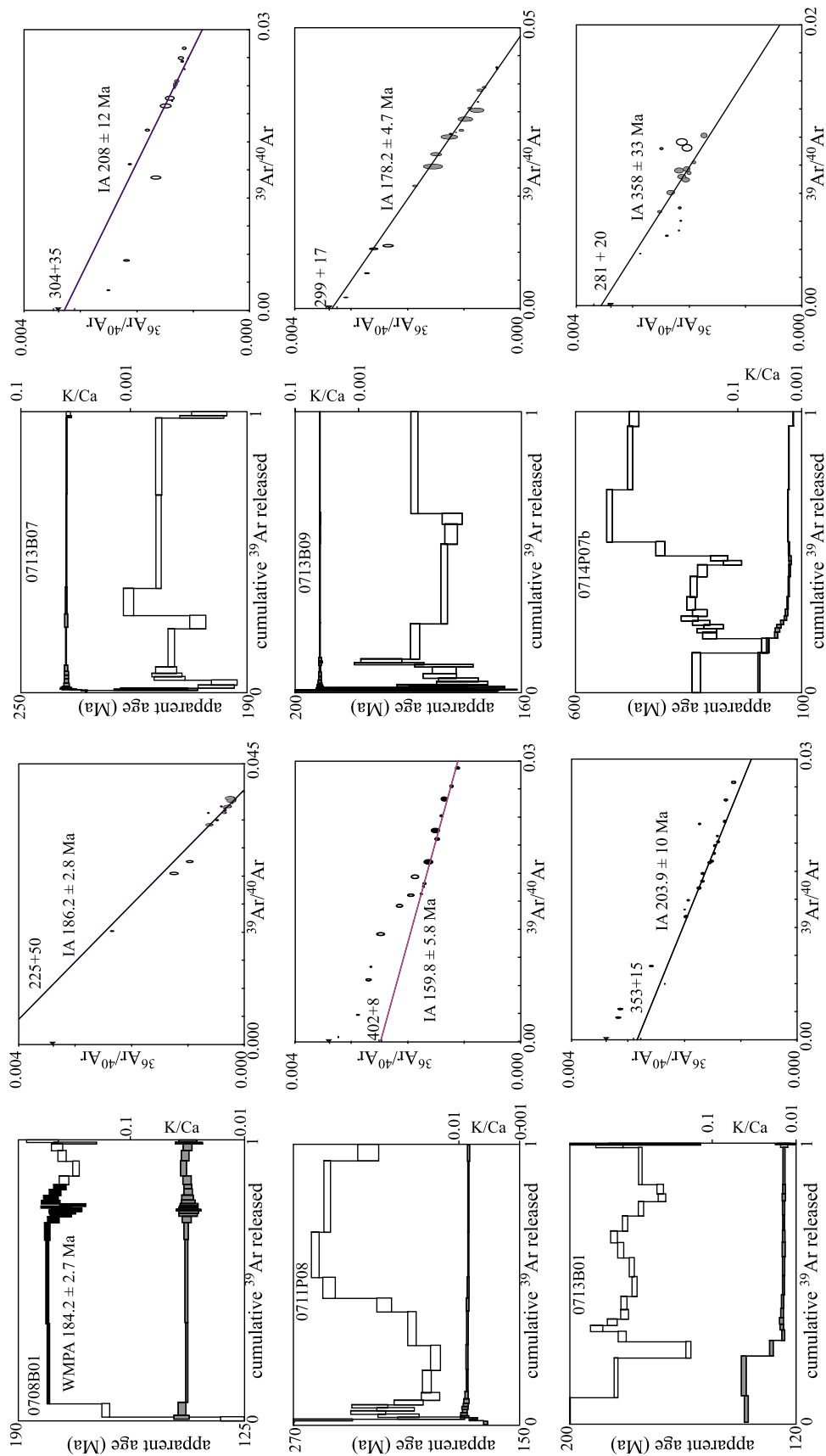


Figure 4. New $^{40}\text{Ar}/^{39}\text{Ar}$ analyses for the Talkeetna arc; homblende unless otherwise noted. Apparent age spectra and K/Ca ratios on left; inverse isochron diagrams on right. Age and K/Ca spectra show 1σ uncertainties excluding error in irradiation parameter J . WMPA, weighted mean plateau age; filled steps included in age calculation. IA, isochron age; gray isotopic ratios excluded from age calculation. Age uncertainties are 2σ and include uncertainty in monitor age and decay constant. Triangles on vertical axis of isochron diagrams show $^{40}\text{Ar}/^{36}\text{Ar}$ composition of Earth's atmosphere. Calculations and figures produced with *Isoplot* [Ludwig, 2003].

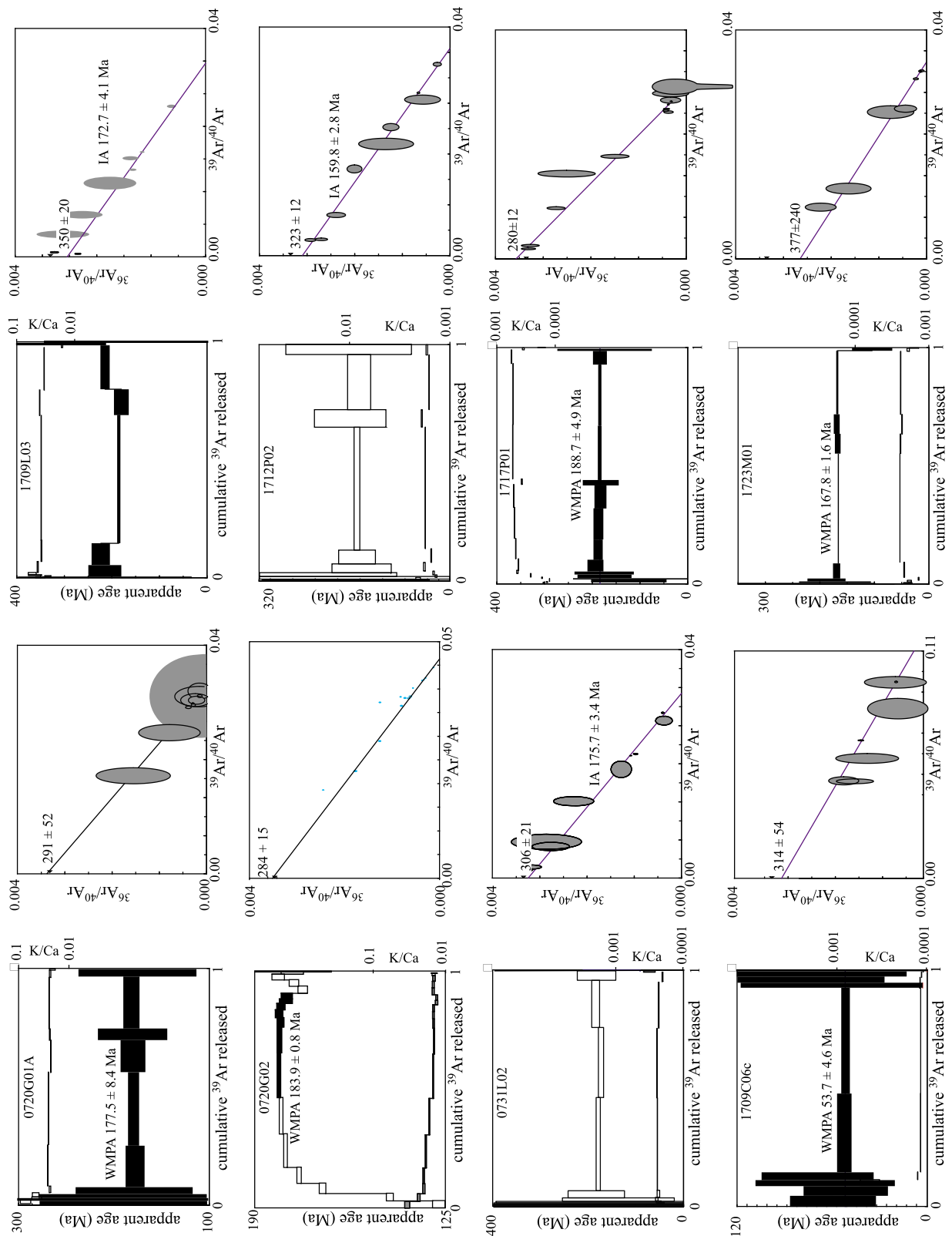


Figure 4. (continued)

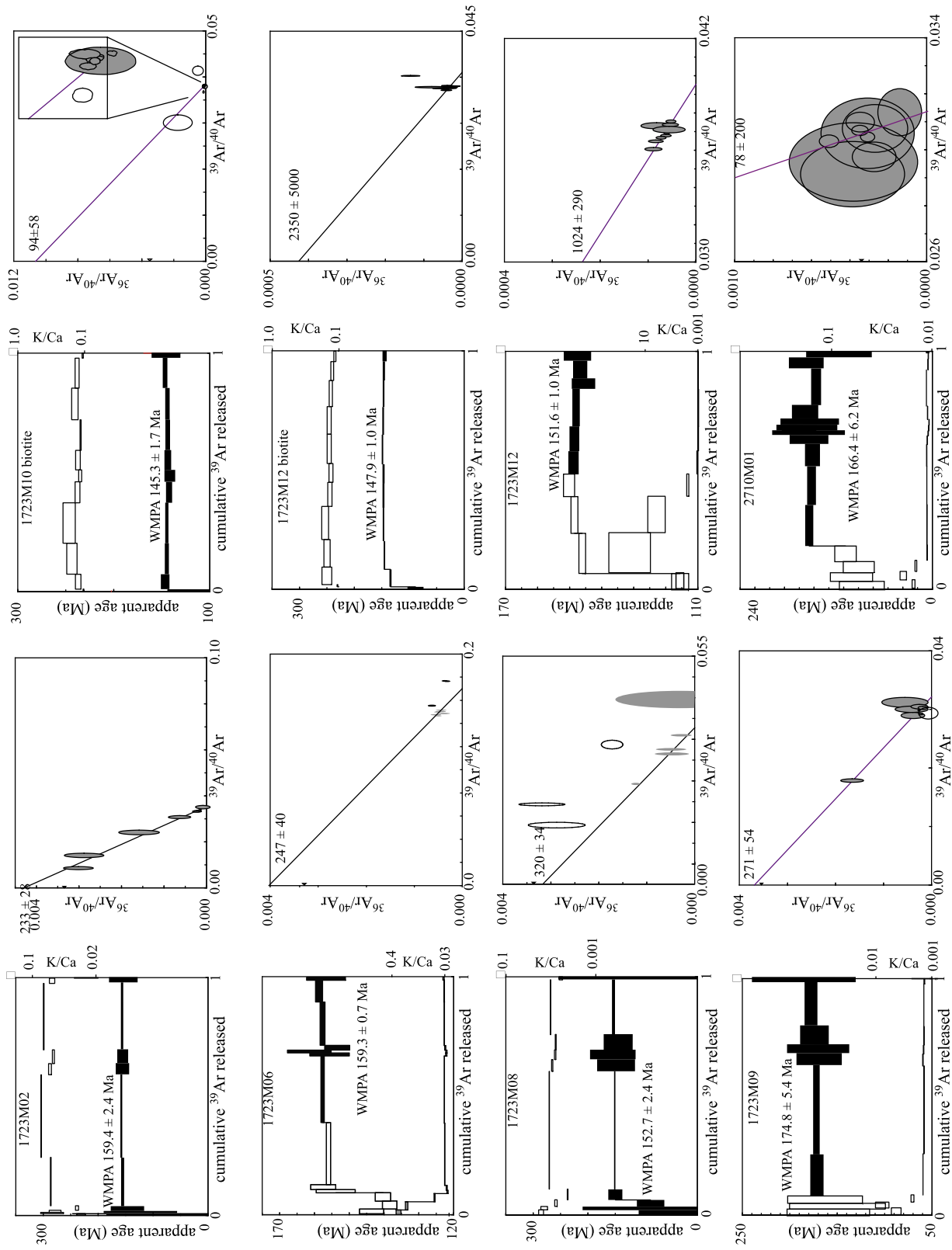


Figure 4. (continued)

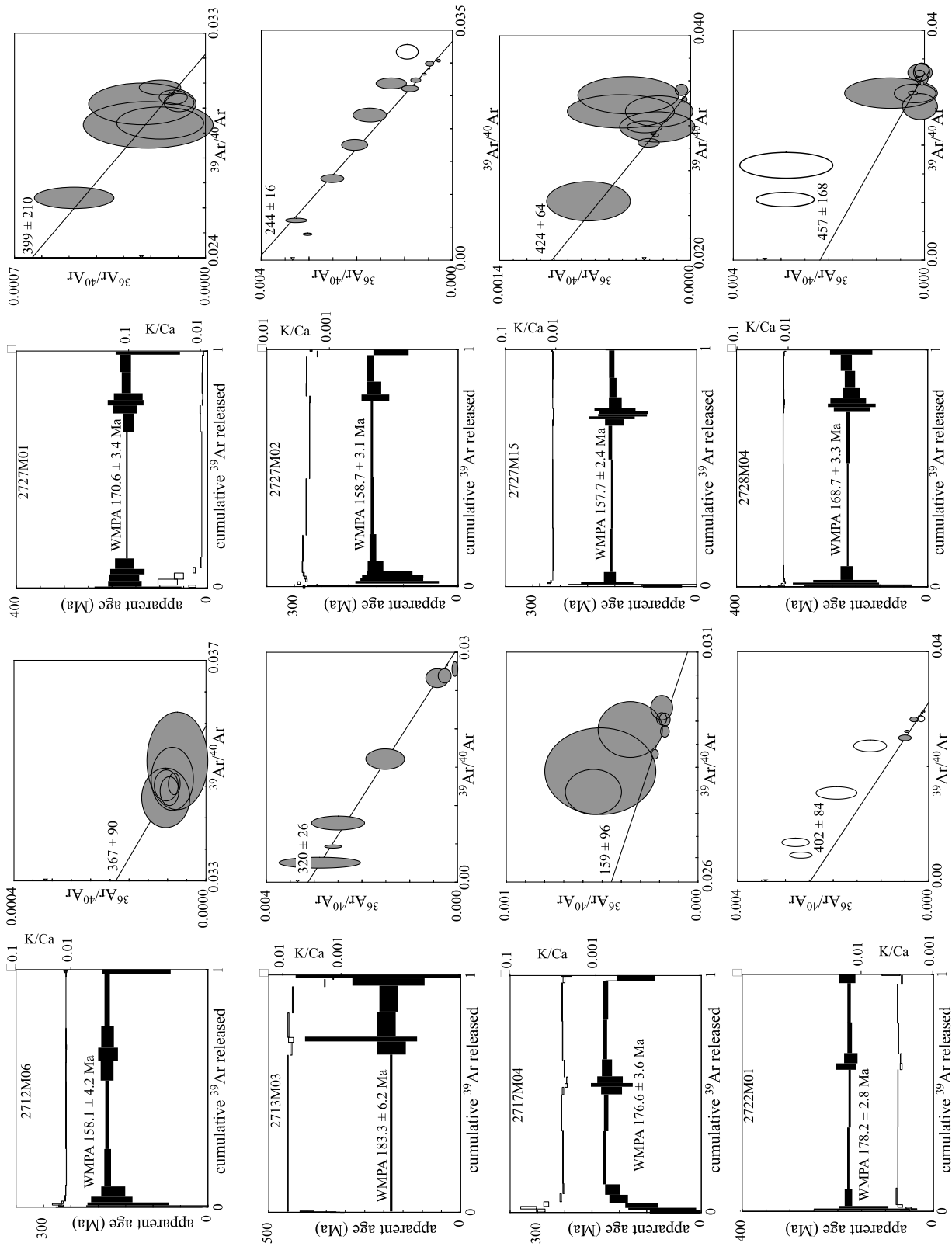


Figure 4. (continued)

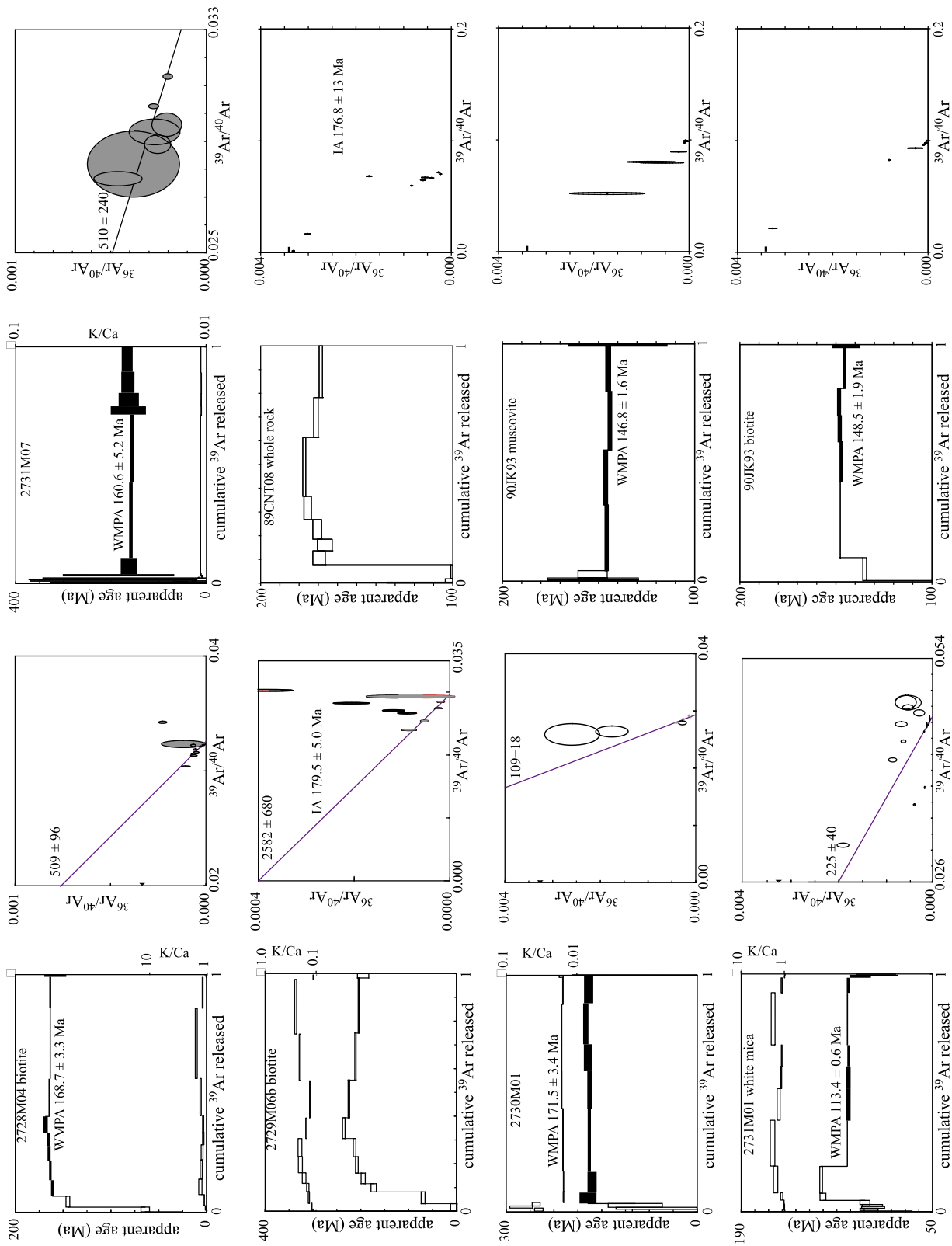


Figure 4. (continued)

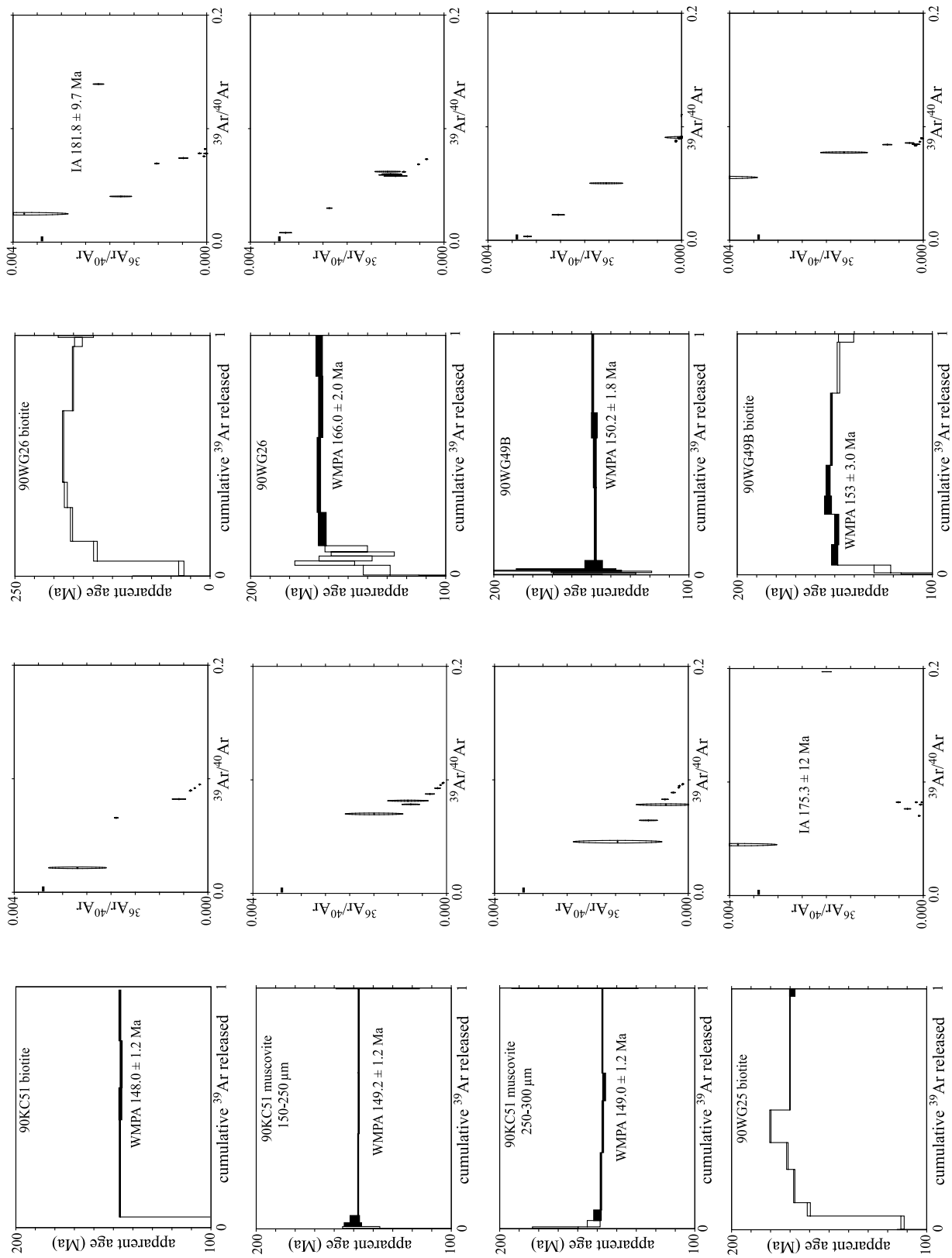


Figure 4. (continued)

Table 4. U-Th/He Data^a

Sample Name	ncc ⁴ He	ng U	ng Th	Ft	Corrected Age (Ma)	±2σ	Radius (um)	Mass (ug)	U (ppm)	Th (ppm)	Th/U	He (STP ncc/mg)
<i>Apatite</i>												
0718P01Baa	0.19	0.05	0.08	0.632	38.2	2.3	33.5	1.33	35.0	63.0	1.80	146
0718P01Bab	0.08	0.02	0.08	0.635	26.4	1.6	37.5	1.23	15.3	63.5	4.15	61.6
					32 ± 18							
1724M01aa	0.01	0.01	0.01	0.616	9.79	0.6	34.5	0.95	6.08	10.8	1.77	6.29
1724M01aa	0.01	0.01	0.02	0.645	9.52	0.6	38.5	1.23	6.11	13.7	2.24	6.94
					9.7 ± 0.4							
0731L02a	0.39	0.38	0.43	0.708	9.41	0.75	35.5	3.06	124	140	1.13	
0731L02b	0.33	0.41	0.36	0.643	8.68	0.69	28.5	1.52	267	239	0.90	
					9.0 ± 0.5							
<i>Zircon</i>												
0718P01Bza	7.79	0.64	0.14	0.697	137	11	31.8	2.80	228	49.0	0.21	2781
0720G02za	14.18	1.45	0.54	0.762	97.0	7.8	40.8	6.66	218	81.7	0.37	2129
0720G02zb	5.97	0.62	0.16	0.761	98.8	7.9	42.8	5.70	108	28.4	0.26	
					97.8 ± 5.5							
1719L02a	0.68	0.13	0.01	0.772	56.1	4.5	45	6.41	19.8	2.33	0.12	107
1719L02b	4.00	0.67	0.06	0.767	63.0	5.0	42.3	6.20	108	9.8	0.09	645
					59 ± 10							
1721M01a	9.76	0.74	0.33	0.748	131	10	41.5	4.69	158	71.0	0.45	2081
1721M01b	28.2	2.06	0.77	0.796	130	10	45.5	14.34	143	53.7	0.37	1970
					130 ± 7							
1721M05a	13.8	1.64	0.59	0.822	77.9	6.2	53.8	19.67	83.3	29.7	0.36	701
1721M05b	1.08	0.14	0.07	0.758	74.6	6.0	39.9	6.94	20.2	10.3	0.51	155
					76.2 ± 4.3							
1723M09a	27.9	2.34	0.60	0.790	117	9.4	46.3	9.96	234	59.9	0.26	2798
1723M09b	35.4	2.80	0.84	0.796	122	9.7	50.8	9.41	298	89.6	0.30	3761
					119 ± 7							
1723M12a ^b	62.2	4.14	0.97	0.894	131	10	96	82.84	50.0	11.7	0.23	750
1723M12b ^c	33.6	2.40	0.56	0.857	127	10	69.3	33.97	70.7	16.5	0.23	988
					129 ± 7							
2714M02a	10.6	1.22	0.31	0.743	90.9	7.3	41	4.25	287	73.5	0.26	2491
2714M02b	23.8	2.16	0.76	0.731	115	9.2	37.8	3.91	552	194	0.35	6088
2714M02c	11.33	1.14	0.32	0.706	108	8.7	32.3	3.34	342.4	95.5	0.28	3391
					111 ± 6 (rejecting youngest)							
JMM01a	9.85	0.95	0.32	0.793	100	8.0	48.5	9.67	97.8	33.3	0.34	1018
JMM01b ^d	8.61	0.80	0.33	0.713	114	9.1	32.8	3.93	203	84.5	0.42	2192

^aHere ncc, 10⁻¹² cm³; Ft, alpha ejection correction [Farley, 2002].

^bFour reextracts required.

^cThree reextracts required.

^dNo HNO₃; excess HF in initial dissolution.

[18] A group of ⁴⁰Ar/³⁹Ar and K-Ar hornblende ages in the Chugach Mountains that are spatially associated with the zircon-bearing plutonic rocks range from ~194 Ma to ~160 Ma; except for 3 outliers, the bulk of these ages are older than ~170 Ma. These ages have no relation to paleo-depth in the arc. There are four K-Ar biotite ages of ~170 Ma [Winkler, 1992], indicating that either the younger hornblende ages were partially reset or that the biotites have excess ⁴⁰Ar. All of these data are likely affected, to an unknown extent, by the 140–135 Ma (?) western Chugach magmatism (see references above and discussion below). These data suggest that, at the regional scale, the Talkeetna arc in the Chugach Mountains had reached temperatures <300°C–500°C by ~160 Ma, cooling at an average rate of >10 K/Myr; two old zircon fission track ages are compatible with this inference. This cooling may have been associated with the tectonism recorded by the Naknek Formation in the Talkeetna Mountains [Trop *et al.*, 2005] (see below).

[19] U-Pb zircon, ⁴⁰Ar/³⁹Ar hornblende, ⁴⁰Ar/³⁹Ar mica, and U-Th/He zircon ages from *individual* samples (Figure 6) reveal cooling histories in higher fidelity. In particular, two of the Chugach Mountains samples (2710M01 and 2717M04) cooled at a moderate rate (5–9 K/Myr) from crystallization to <500°C, and one (0720G02) cooled at a rapid rate (75 K/Myr) to <500°C. Similar age differences between U-Pb zircon and ⁴⁰Ar/³⁹Ar hornblende ages of samples separated by <1 km (yellow callouts of Figure 5) suggest that these inferences apply to much of the Chugach Mountains. U-Th/He ages of 39 Ma to 9 Ma from individual samples show that cooling to <200°C varied considerably from 3 to 12 K/Myr.

[20] Our new ⁴⁰Ar/³⁹Ar data shed no additional light on the 140–135 Ma (?) resurgence of magmatism in the westernmost Chugach that was recognized by Pavlis [1983] and Barnett *et al.* [1994] on the basis of 136–130 Ma hornblende ages. The clear 10–20 Myr interregnum between the hornblende ages from the Talkeetna arc and this westernmost

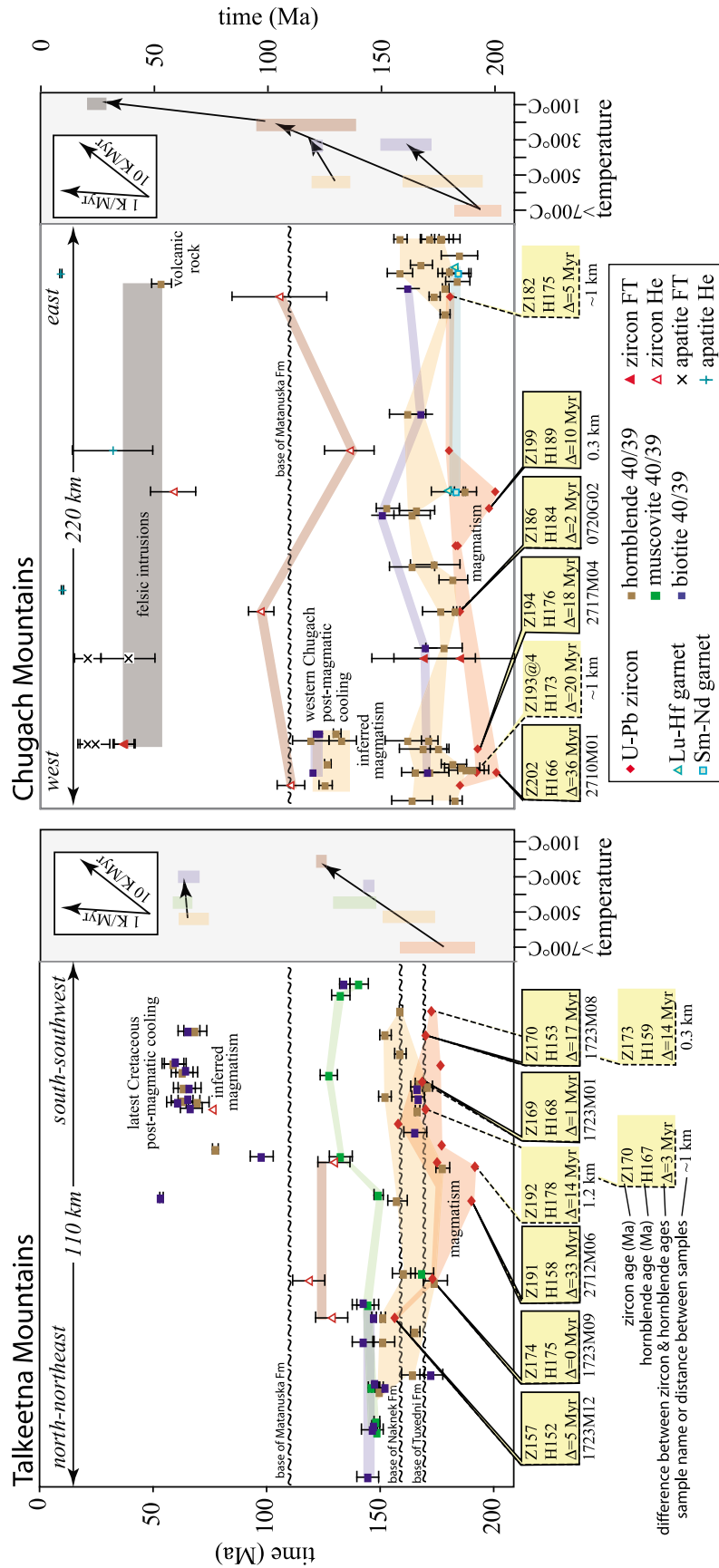


Figure 5. Chronology profiles through the Talkeetna and Chugach mountains. Colored swaths join ages of similar type and age range as aids to visualizing intrusive and cooling histories. Gray panels to the right of each section show regional cooling rates of ~1–10 K/Myr using same colored swaths. Yellow callouts at bottom show differences between zircon U-Pb and hornblende ages; callouts with solid borders are from individual named samples, whereas those with dotted borders are from samples separated by indicated distances. Three questionable ages from Figure 1 are not shown, nor are ages from the Chugach terrane.

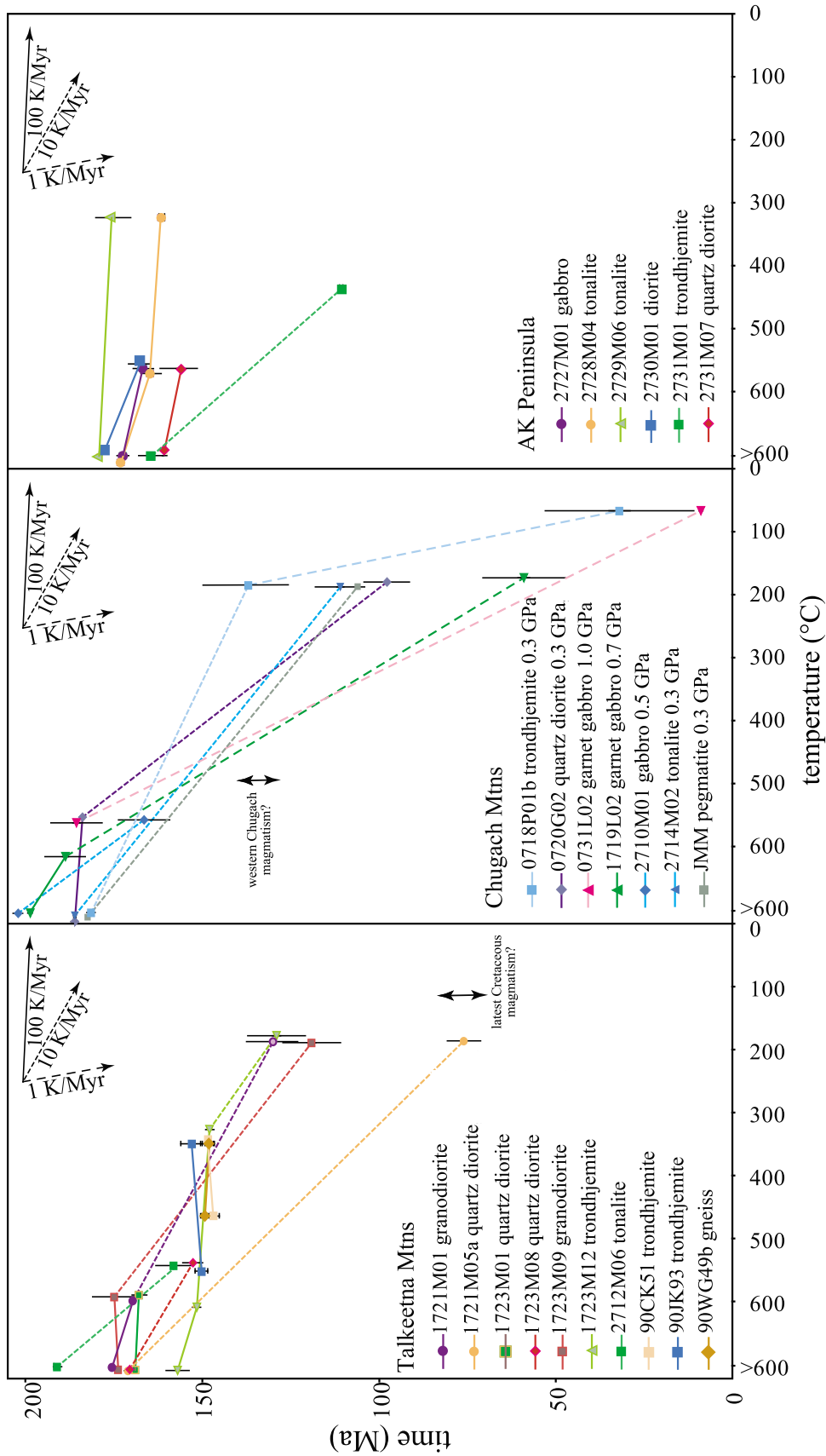


Figure 6. Cooling histories of individual samples determined by U-Pb zircon, $^{40}\text{Ar}/^{39}\text{Ar}$ hornblende, $^{40}\text{Ar}/^{39}\text{Ar}$ mica, (U-Th)/He zircon, and (U-Th)/He apatite ages. Closure temperatures for hornblende and He in zircon based on grain size in thin section and cooling rate. Approximate (re)crystallization pressures of Chugach samples based on the work by Hacker *et al.* [2008]. “Sample” 1719L02 composed of three samples separated by <250 m.

Chugach implies that the two are unrelated, distinct magmatic events. The U-Th/He age from this area is similar to two others farther east in the Chugach Mountains, implying regional cooling to He loss in zircon by ~110 Ma. Widespread zircon U-Th/He ages of 137–99 Ma show that the Oligocene felsic magmatism [e.g., *Little and Naeser*, 1989] had minor impact on the regional thermal gradient, and U-Th/He apatite ages of 32–9 Ma document slow cooling (~1 K/Myr) in the Chugach Mountains at the regional scale.

8.2. Talkeetna Mountains

[21] The U-Pb zircon ages in the Talkeetna Mountains are generally younger than those in the Chugach Mountains (Figures 1 and 5). In detail, U-Pb zircon ages from plutonic rocks in the eastern and central Talkeetna Mountains range from ~178–153 Ma and are interpreted to reflect a northward shift in arc magmatism at ~180 Ma [*Rioux et al.*, 2007]. The plutonic rocks in the western Talkeetna Mountains are ~190 Ma, contain inherited Carboniferous-Triassic zircon and have lower whole-rock initial $^{143}\text{Nd}/^{144}\text{Nd}$ ratios than the rest of the arc, likely reflecting magmatism within the adjacent Wrangellia terrane or interaction between the Talkeetna arc and the Wrangellia terrane [*Rioux et al.*, 2007].

[22] A group of $^{40}\text{Ar}/^{39}\text{Ar}$ and K-Ar hornblende ages in the Talkeetna Mountains that are spatially associated with the zircon-bearing plutonic rocks range from ~175 Ma to ~150 Ma, generally ~10–15 Myr younger than in the Chugach Mountains. Deformation and partial exhumation of the Talkeetna Mountains plutonic suite at this time is recorded by the Naknek Formation that unconformably overlies the Talkeetna Formation [*Trop et al.*, 2005]. There are four K-Ar and $^{40}\text{Ar}/^{39}\text{Ar}$ biotite ages that are older than most of the hornblendes; either the younger hornblende ages were partially reset, the biotites have excess ^{40}Ar , or there are screens of older basement present. A suite of new $^{40}\text{Ar}/^{39}\text{Ar}$ mica ages from 149 to 143 Ma and three new U-Th/He ages of 130–119 Ma imply cooling of the eastern Talkeetna Mountains at ~10 K/Myr. All of these data are likely affected, to an unknown extent, by the 80–70 Ma (?) magmatism implied by the swarm of 70–60 Ma hornblende, muscovite, and biotite $^{40}\text{Ar}/^{39}\text{Ar}$ and K-Ar ages [*Plafker et al.*, 1989].

[23] U-Pb zircon, $^{40}\text{Ar}/^{39}\text{Ar}$ hornblende, $^{40}\text{Ar}/^{39}\text{Ar}$ mica, and U-Th/He zircon ages from *individual* samples (Figure 6) reveal cooling histories in higher fidelity. In particular, three of the Talkeetna Mountains samples (1723M01, 1723M09, and 1723M12) cooled rapidly (>20 K/Myr) from crystallization to <500°C, and two (1723M08 and 2712M06) cooled at a moderate rate (5–9 K/Myr) to <500°C. Subsequent cooling to <400°C was rapid for all samples, and to 200°C for three of four samples. Similar age differences between U-Pb zircon and $^{40}\text{Ar}/^{39}\text{Ar}$ hornblende ages of samples separated by <1.2 km (yellow callouts of Figure 5) suggest that these inferences apply to much of the Talkeetna Mountains.

8.3. Alaska Peninsula

[24] U-Pb zircon ages show that the Talkeetna arc in the Alaska Peninsula crystallized over the interval from 183 Ma

to 164 Ma [*Rioux et al.*, 2010], similar to the 177–159 Ma magmatism in the Talkeetna Mountains; two ages from the Kodiak archipelago are significantly older, at 213 Ma and 217 Ma [*Rioux et al.*, 2010]. Hornblende $^{40}\text{Ar}/^{39}\text{Ar}$ ages are on average 5–10 Myr younger than the U-Pb zircon ages, ranging from 171.7 ± 3.4 Ma to 157.8 ± 2.4 Ma, again similar to the Talkeetna Mountains. There are two biotite ages of 179.5 ± 5.0 Ma and 165.5 ± 0.8 Ma, and a muscovite age of 113.3 ± 0.6 Ma. U-Pb zircon, $^{40}\text{Ar}/^{39}\text{Ar}$ hornblende and mica ages from *individual* samples (Figure 6) indicate uniformly rapid cooling rates of ~100–20 K/Myr (except for sample 2731M01).

9. Thermal History of the Talkeetna Arc

[25] In a gross sense, the magmatism in the Chugach Mountains spanned ~20 Myr and cooling to <300°C was complete within another 20 Myr; the Talkeetna Mountains were magmatically active for longer, 30 Myr, although the older (~190 Ma) magmatism in this area may not be directly related to the Talkeetna arc, and cooled to <300°C in ~20 Myr. The Alaska Peninsula section of the Talkeetna arc was active for 20 Myr and cooled to <300°C within 6 Myr.

[26] In detail, however, the crystallization and cooling histories of different portions of the arc show considerable variability, even for something as simple as the time interval between igneous crystallization (i.e., the zircon U-Pb age) and cooling below ~550°C (i.e., the hornblende age) (Figures 5 and 7). In the Chugach Mountains, individual samples ($n = 3$) and samples from nearby outcrops ($n = 3$) record zircon-hornblende age differences of 2 Myr to 36 Myr. In the Talkeetna Mountains, zircon-hornblende pairs differ by 0 Myr to 33 Myr (five individual samples and three sets of nearby samples); these are maxima, as partial resetting of hornblende by later magmatism is likely. Four zircon-hornblende pairs for the Alaska Peninsula section differ by 4–11 Myr (Figure 2). Thus, whereas some parts of the arc cooled below hornblende closure temperatures during active magmatism, other portions of the arc, particularly in the Chugach and Talkeetna mountains, remained hot (>500°C) well after the termination of magmatism. The longest zircon-hornblende cooling intervals come from the oldest parts of the arc, and the youngest parts of the arc have relatively short cooling intervals. The cooling rates show no dependence on depth, based on the pressures reported by *Hacker et al.* [2008].

[27] It is important to note that this thermal history is strongly biased by the depth-dependent compositional variation of the arc, which dictates the type of chronometers that can be used at each depth. Specifically, based on the reconstruction by *Hacker et al.* [2008], the zircon U-Pb and U-Th/He ages come principally from rocks that are interpreted to have crystallized at pressures of 0.4–0.7 GPa, the garnet ages come from rocks (re)crystallized at 0.7 and 1.0 GPa, the hornblende and mica ages are chiefly from rocks (re)crystallized at 0.4–0.7 GPa. In effect then, we have good cooling rate data for depths of ~13–24 km, but deeper and shallower depths are not well constrained. Moreover, because the arc grew to ~35 km thickness within what we presume was 7 km thick oceanic crust, the rocks now at 13–

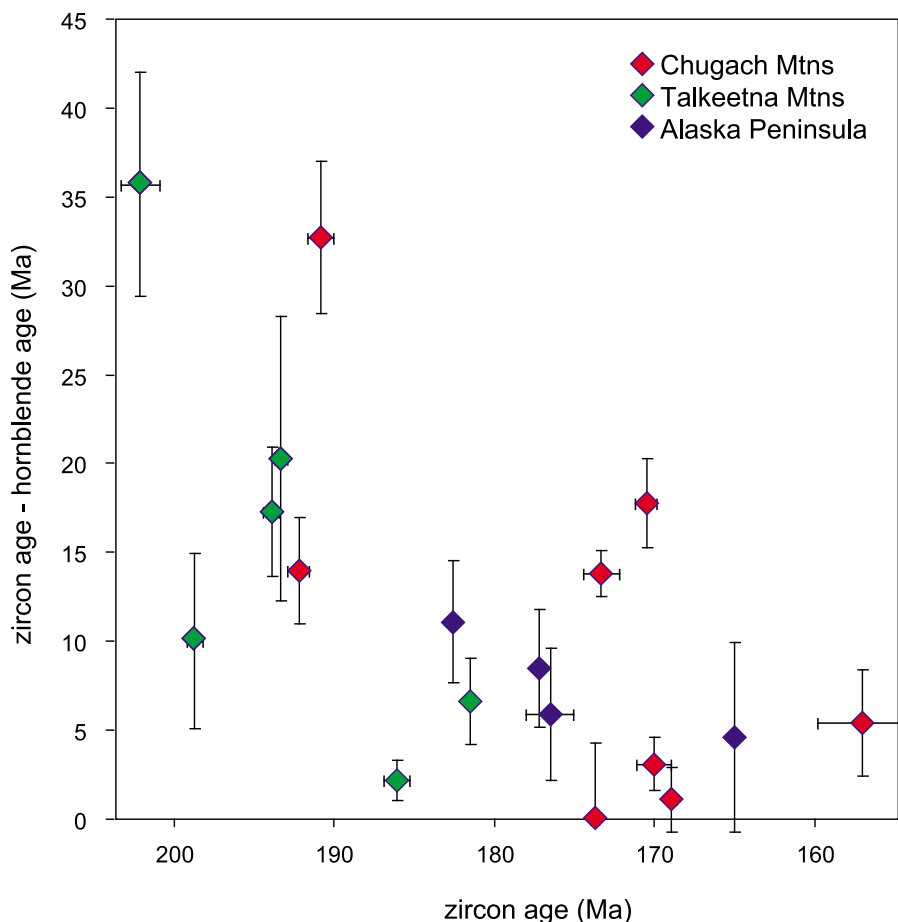


Figure 7. The time gaps between U-Pb zircon crystallization ages and $^{40}\text{Ar}/^{39}\text{Ar}$ hornblende cooling ages range from 36 Myr to 0 Myr, with the biggest gaps for the oldest samples.

24 km depth might have crystallized near the bottom of the arc and been underplated by subsequent intrusions, might have crystallized at subvolcanic depths and been pushed downward, or might even have gone up and down in the crust if the arc underwent (episodic?) extensional or contraction events.

10. Thermal Model of the Talkeetna Arc

[28] Is the spatially variable cooling pattern documented for the midcrustal levels of the Talkeetna arc typical of an intraoceanic arc, or should an intraoceanic arc have a simple monotonic, spatially homogeneous cooling history? Is it possible, for example, that the chaotic cooling pattern of the Talkeetna arc is an artifact of Ar loss during younger events? With the limitations and ambiguities listed in the previous paragraph in mind, we can assess this question.

10.1. Model Setup

[29] We used a simple, 1D thermal model to examine whether the spatially variable thermochronological signature of the Talkeetna arc is “normal” for an arc. Models judged to be successful were those that match the thermo-

chronologic record, reproduce the PT conditions reported by Hacker *et al.* [2008], and have heat flow typical of an intraoceanic arc: 50–70 mW/m² [Wada and Wang, 2009]. The code was built around that of Hinojosa and Mickus [2002].

[30] For simplicity, the model uses fixed values of density = 3000 kg/m³, thermal conductivity = 2.3 W/mK [Kelemen *et al.*, 2003a], and heat capacity = 1.3 J/gK [Leth-Miller *et al.*, 2003], with a resulting thermal diffusivity of 0.6E-6 m²/s. Radiogenic heat production rate is set to 0.4 uW/m³ in the felsic portion of the crust following bulk compositions reported for the Talkeetna arc [Kelemen *et al.*, 2003a].

[31] The initial thermal state, chosen to represent instantaneous formation of an arc within existing oceanic lithosphere, was 10 Myr old oceanic lithosphere [Stein and Stein, 1992] down to a depth of 17 km (i.e., normal crustal thickness +10 km of mantle lithosphere), underlain by asthenosphere at 1350°C. (Within a reasonable range of temperatures, the asthenosphere temperature made little difference to the model results.)

[32] Each model run began with 7 km of oceanic crust. Over the first 20 Myr of the model, 5 km of volcanic rocks were erupted onto the top of the crust at a constant rate, and

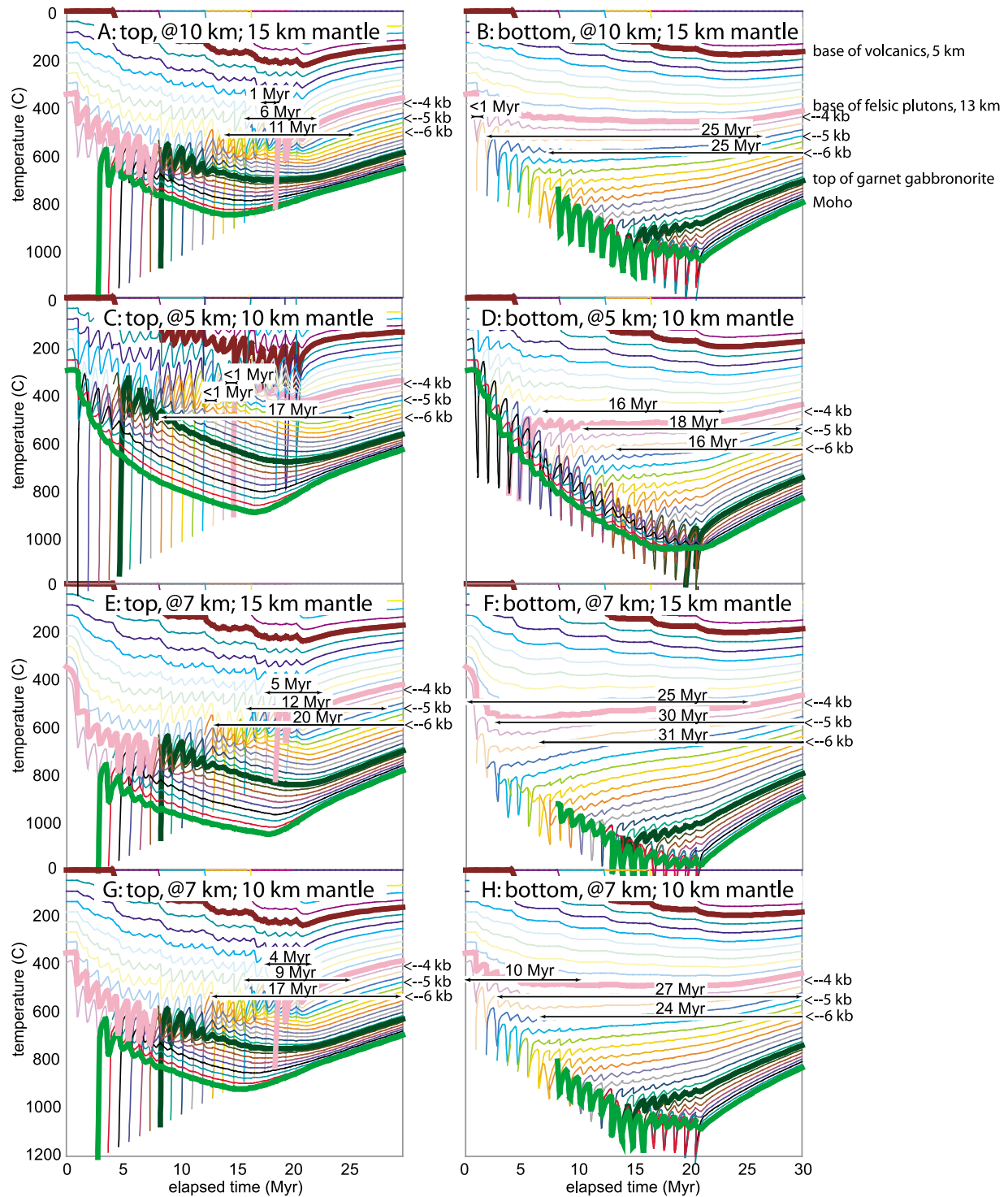


Figure 8. (left and right) Modeled temperature evolution of 1 km depth intervals. Models in which plutons are intruded at the bottom of the section (Figure 8, right) show relatively simple thermal histories in which plutonic rocks are hottest when intruded and cool ever after and mostly large zircon-hornblende age differences in the 0.4–0.6 GPa depth interval (black arrows). Models in which plutons are intruded at the top of the section (Figure 8, left) show complicated thermal behavior, with intrusion-driven oscillations, inversions, and heating of previously crystallized intrusions, and a broad range of zircon, hornblende age differences (black arrows); this is similar to the Talkeetna arc. Captions for each of the eight panels indicate whether each pluton is intruded at the top or bottom of the section, the initial thickness of the plutonic section, and the thickness of the mantle lithosphere.

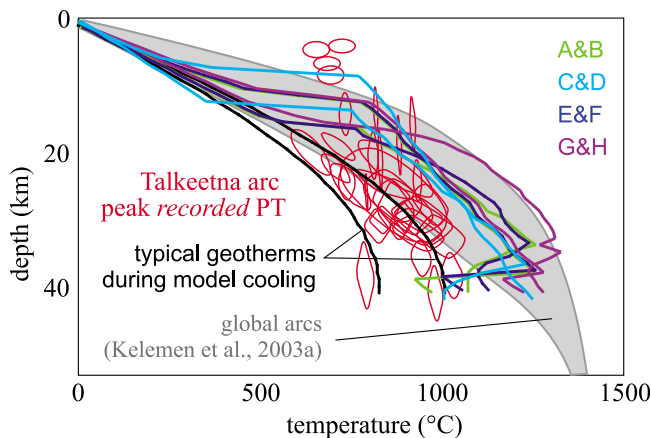


Figure 9. Maximum P-T conditions in each model at 1 km depth intervals (colored lines), typical cooling conditions of the models (black lines), and peak recorded PT conditions from the Talkeetna arc [Hacker *et al.*, 2008]. One of the models produced temperatures high enough to satisfy the PT conditions at the top of the Talkeetna section, and all produced temperatures higher than the peak recorded PT conditions.

22 km of plutonic rocks were intruded into the crust. This produced a model arc similar to the Talkeetna arc with its 5 km of volcanic rocks, 8 km of felsic plutons, 13 km of mafic plutons, and 8 km of basal garnet gabbro [Hacker *et al.*, 2008]. The volcanic rocks were assigned a temperature of 0°C to reflect eruption in the atmosphere or ocean. The plutonic rocks were intruded into the crustal section via two end-member modes, either (1) at a constant depth of 5, 7 or 10 km (such that the “oldest” plutons ended up at the bottom of the pile) or (2) beginning at a depth of 5, 7 or 10 km and moving downward (such that the oldest plutons ended up at the top of the pile). The plutons are each 1 km thick and were intruded at temperatures of 1250°C (gabbro) to 950°C (intermediate compositions); crystallization of each pluton generated latent heat of 400 kJ/kg. Intrusion of the plutons at a constant rate is a reasonable representation of the existing zircon U-Pb age data set, which is compatible with relative uniform magmatic flux over a 20 Myr period. The thickness of the mantle lithosphere was maintained at 10 or 15 km for the first 20 Myr. After 20 Myr, the entire section was allowed to cool.

10.2. Model Results

[33] The thermal evolution of 1 km depth intervals for eight different runs are shown in Figure 8. Models in which intrusions are always emplaced at the bottom of the plutonic section (Figure 8, right) show relatively simple thermal histories in which the temperature always increases downward within the growing arc. Each pluton that is intruded undergoes near-monotonic cooling, aside from initial minor thermal oscillations produced by nearby intrusions. *Peak* temperatures increase slowly at shallow depths, but are hotter at deeper levels (Figure 9). All four of these models

show chiefly large differences between the time that the pluton intruded (i.e., the predicted U-Pb zircon age) and the time that the pluton cooled through ~550°C (i.e., the predicted hornblende age) (black arrow in Figure 8). These model results are generally unlike the cooling history of the Talkeetna arc.

[34] Models in which intrusions are always emplaced at the top of the plutonic section (Figure 8, left) show more complicated thermal histories. Each pluton that is intruded is initially quenched, but then undergoes heating produced by nearby intrusions; shallow levels of the plutonic section cool only once plutonism stops at 20 Myr. *Peak* temperatures increase rapidly at shallow depths, but are cooler at deeper levels (Figure 9). All four of these models show small (<1 Myr) to large differences in (20 Myr) in the time that the pluton intruded (i.e., the predicted U-Pb zircon age) and the time that the pluton cooled through ~550°C (i.e., the predicted hornblende age) (black arrow). These model results are more like the Talkeetna arc.

[35] These models illuminate simple facts: Intrusions that remain near the base of an arc can experience high temperatures as long as the arc is active, leading to large differences in zircon crystallization and hornblende cooling ages. Intrusions emplaced at shallow levels in an arc can cool rapidly, leading to undetectable differences in zircon crystallization and hornblende cooling ages. At intermediate levels, a range of zircon-hornblende age differences are expected. Thus, the spatially variable cooling histories documented for the Talkeetna arc are entirely reasonable and may be characteristic of arcs worldwide. Note that any episodicity in magmatism, spatial variation in magmatic flux, or deformation of the arc will serve to introduce even more variability.

11. Conclusions

[36] New Lu-Hf and Sm-Nd garnet ages, $^{40}\text{Ar}/^{39}\text{Ar}$ hornblende, mica and whole-rock ages, and U-Th/He zircon and apatite ages show that the Talkeetna arc of Alaska had a spatially variable cooling history. The main period of arc magmatism was dated by the U-Pb zircon method [Rioux *et al.*, 2007, 2010] as 202–181 Ma in the Chugach Mountains, and 183–153 Ma in the eastern Talkeetna Mountains and Alaska Peninsula. New Lu-Hf and Sm-Nd ages of ~184 Ma and ~182 Ma for igneous and metamorphic garnet indicate that deeper (25–35 km depths) sections of the arc in the Chugach Mountains remained above ~700°C for as much as 15 Myr. $^{40}\text{Ar}/^{39}\text{Ar}$ hornblende ages, presumed to record cooling below ~500°C–575°C, are chiefly 194–170 Ma in the Chugach Mountains and 175–150 Ma in the Talkeetna Mountains and Alaska Peninsula. They differ from U-Pb zircon ages in the same samples by as little as 0 Myr and as much as 36 Myr, indicating that postcrystallization cooling was rapid (100 K/Myr) in some locations and slow (<10 K/Myr) in others, likely reflecting repeated reheating events. $^{40}\text{Ar}/^{39}\text{Ar}$ muscovite and biotite ages associated with the arc range from ~180 Ma to 130 Ma, although a group of older muscovite ages in the northeastern Talkeetna Mountains span a narrower range of 150–143 Ma. There is a

similar range in U-Th/He zircon ages, but the oldest are ~137 to 129 Ma.

[37] Local Cretaceous and Oligocene magmatism means that some of these cooling ages, particularly those with lower closure temperatures, were probably partially reset. Even so, the differences in zircon, garnet and hornblende ages, in particular, imply that the thermal history of the Talkeetna arc was spatially variable. The range in U-Pb zircon ages implies a protracted crystallization history for the arc, so perhaps it is not surprising that the thermal his-

ories of different parts of the arc were different. Thermal models demonstrate that spatial variation in cooling rates is expected in the intermediate crustal levels of an intraoceanic arc, such that there is no need to call upon episodic magmatism, deformation or subsequent thermal events to explain the observed cooling history of the Talkeetna arc.

[38] **Acknowledgments.** Thanks to Calvin Barnes and George Bergantz for reviews. This was funded by NSF EAR-9910899.

References

- Amato, J. M., M. E. Rioux, P. B. Kelemen, G. E. Gehrels, P. D. Clift, T. L. Pavlis, and A. E. Draut (2007), U-Pb geochronology of volcanic rocks from the Jurassic Talkeetna Formation and detrital zircons from prearc and postarc sequences: Implications for the age of magmatism and inheritance in the Talkeetna arc, *Spec. Pap. Geol. Soc. Am.*, *431*, 253–271.
- Barnett, D. E., J. R. Bowman, T. L. Pavlis, J. R. Rubenstone, L. W. Sneek, and T. C. Onstott (1994), Metamorphism and near-trench plutonism during initial accretion of the Cretaceous Alaskan forearc, *J. Geophys. Res.*, *99*, 24,007–24,024, doi:10.1029/94JB02462.
- Burns, L. E. (1985), The Border Ranges ultramafic and mafic complex, south-central Alaska: Cumulate fractionates of island arc volcanics, *Can. J. Earth Sci.*, *22*, 1029–1038.
- Calvert, A. T., P. B. Gans, and J. M. Amato (1999), Diapiric ascent and cooling of a sillimanite gneiss dome revealed by $^{40}\text{Ar}/^{39}\text{Ar}$ thermochronology: The Kigluak Mountains, Seward Peninsula, Alaska, in *Exhumation Processes: Normal Faulting, Ductile Flow, and Erosion*, edited by U. Ring et al., pp. 205–232, Geol. Soc. of London, London.
- Clift, P. D., A. E. Draut, P. B. Kelemen, J. Blusztajn, and A. Greene (2005), Stratigraphic and geochemical evolution of an oceanic arc upper crustal section: The Jurassic Talkeetna Volcanic Formation, south-central Alaska, *Geol. Soc. Am. Bull.*, *117*, 902–925, doi:10.1130/B25638.1.
- Csejtesy, B. Jr., W. H. Nelson, D. L. Jones, N. J. Silberling, R. M. Dean, M. S. Morris, M. A. Lanphere, J. G. Smith, and M. L. Silberling (1978), Reconnaissance geologic map and geochronology, Talkeetna Mountains quadrangle, northern part of Anchorage quadrangle, and southwest corner of Healy quadrangle, Alaska, *U.S. Geol. Surv. Open File Rep.*, 78-558A.
- DeBari, S. M., and R. G. Coleman (1989), Examination of the deep levels of an island arc: Evidence from the Tonsina ultramafic-mafic assemblage, Tonsina, Alaska, *J. Geophys. Res.*, *94*, 4373–4391, doi:10.1029/JB094iB04p04373.
- Drake, J., and P. W. Layer (2001), $^{40}\text{Ar}/^{39}\text{Ar}$ analyses from the Iron Creek area, *Rep. 2001-3*, 11 pp., Alaska Div. of Geol. and Geophys. Surv., Fairbanks.
- Dunlap, W. J. (2000), Nature's diffusion experiment: The cooling-rate cooling-age correlation, *Geology*, *28*, 139–142, doi:10.1130/0091-7613(2000)28<139:NDETCC>2.0.CO;2.
- Farley, K. A. (2002), (U-Th)/He dating: Techniques, calibrations, and applications, *Rev. Mineral. Geochem.*, *47*, 819–844, doi:10.2138/rmg.2002.47.18.
- Flowers, R. A., R. A. Ketcham, D. L. Shuster, and K. A. Farley (2009), Apatite (U-Th)/He thermochronometry using a radiation damage accumulation and annealing model, *Geochim. Cosmochim. Acta*, *73*, 2347–2365, doi:10.1016/j.gca.2009.01.015.
- Ganguly, J., and M. Tirone (1999), Diffusion closure temperature and age of a mineral with arbitrary extent of diffusion: Theoretical formulation and applications, *Earth Planet. Sci. Lett.*, *170*, 131–140, doi:10.1016/S0012-821X(99)00089-8.
- Gradstein, F. M., J. G. Ogg, and A. G. Smith (2004), *A Geologic Time Scale 2004*, Cambridge Univ. Press, Cambridge, U. K.
- Greene, A. R., S. M. DeBari, P. B. Kelemen, J. Blusztajn, and P. D. Clift (2006), A detailed geochemical study of island arc crust: The Talkeetna Arc section, south-central Alaska, *J. Petrol.*, *47*, 1051–1093, doi:10.1093/petrology/egl002.
- Grove, M., and M. Harrison (1996), $^{40}\text{Ar}^*$ diffusion in Fe-rich biotite, *Am. Mineral.*, *81*, 940–951.
- Hacker, B. R., and Q. Wang (1995), Ar/Ar geochronology of ultrahigh-pressure metamorphism in central China, *Tectonics*, *14*, 994–1006, doi:10.1029/95TC00932.
- Hacker, B. R., L. Mehl, P. B. Kelemen, M. Rioux, M. D. Behn, and P. Luffi (2008), Reconstruction of the Talkeetna intraoceanic arc of Alaska through thermobarometry, *J. Geophys. Res.*, *113*, B03204, doi:10.1029/2007JB005208.
- Harrison, T. M. (1981), Diffusion of ^{40}Ar in hornblende, *Contrib. Mineral. Petrol.*, *78*, 324–331, doi:10.1007/BF00398927.
- Harrison, T. M., J. Celerier, A. B. Aikman, J. Hermann, and M. T. Heizler (2009), Diffusion of ^{40}Ar in muscovite, *Geochim. Cosmochim. Acta*, *73*, 1039–1051, doi:10.1016/j.gca.2008.09.038.
- Hinojosa, J. H., and K. L. Mickus (2002), Thermoelastic modeling of lithospheric uplift: A finite-difference numerical solution, *Comput. Geosci.*, *28*, 155–167, doi:10.1016/S0098-3004(01)00028-0.
- Imlay, R. W. (1984), Early and Middle Bajocian (Middle Jurassic) ammonites from southern Alaska, *U.S. Geol. Surv. Prof. Pap.*, *1322*, 38 pp.
- Jaffey, A. H., K. F. Flynn, L. E. Glendenin, W. C. Bentley, and A. M. Essling (1971), Precision measurement of the half-lives and specific activities of ^{235}U and ^{238}U , *Phys. Rev. C*, *4*, 1889–1906, doi:10.1103/PhysRevC.4.1889.
- Jan, M. Q., and R. A. Howie (1981), The mineralogy and geochemistry of the metamorphosed basic and ultrabasic rocks of the Jijal complex, Kohistan, NW Pakistan, *J. Petrol.*, *22*, 85–126, doi:10.1093/petrology/22.1.85.
- Kelemen, P. B., et al. (2003a), Site 1275, *Proc. Ocean Drill. Program Initial Rep.*, 209, 1–167.
- Kelemen, P. B., J. L. Rilling, E. M. Parmentier, L. Mehl, and B. R. Hacker (2003b), Thermal structure due to solid-state flow in the mantle wedge beneath arcs, in *Inside the Subduction Factory*, *Geophys. Monogr. Ser.*, vol. 138, edited by J. Eiler, pp. 293–311, AGU, Washington, D. C.
- Kirschner, D. L., M. A. Cosca, H. Masson, and J. C. Hunziker (1996), Staircase $^{40}\text{Ar}/^{39}\text{Ar}$ spectra of fine-grained white mica: Timing and duration of deformation and empirical constraints on argon diffusion, *Geology*, *24*, 747–750, doi:10.1130/0091-7613(1996)024<0747:SAASOF>2.3.CO;2.
- Kylander-Clark, A. R. C., B. R. Hacker, C. M. Johnson, B. L. Beard, N. J. Mahlen, and T. J. Lapen (2007), Timing of multi-stage metamorphism during ultrahigh-pressure continental subduction and exhumation: Lu/Hf and Sm/Nd geochronology in western Norway, *Chem. Geol.*, *232*, 137–154.
- Kylander-Clark, A. R. C., B. R. Hacker, C. M. Johnson, B. L. Beard, and N. J. Mahlen (2009), Slow subduction of a thick ultrahigh-pressure terrane, *Tectonics*, *28*, TC2003, doi:10.1029/2007TC002251.
- Leth-Miller, R., A. D. Jensen, P. Glarborg, L. M. Jensen, P. B. Hansen, and S. B. Jørgensen (2003), Experimental investigation and modelling of heat capacity, heat of fusion and melting interval of rocks, *Thermochim. Acta*, *406*, 129–142, doi:10.1016/S0040-6031(03)00248-X.
- Little, T. A., and C. W. Naeser (1989), Tertiary tectonics of the Border Ranges fault system, Chugach Mountains, Alaska: Deformation and uplift in a forearc setting, *J. Geophys. Res.*, *94*, 4333–4359, doi:10.1029/JB094iB04p04333.
- Ludwig, K. R. (2003), *Isoplot 3.00: A Geochronological Toolkit for Microsoft Excel*, vol. 4, 74 pp., Berkeley Geochronol. Cent. Spec. Publ., Berkeley, Calif.
- Lugmair, G. W., and K. Marti (1978), Lunar initial $^{143}\text{Nd}/^{144}\text{Nd}$: Differential evolution of the lunar crust and mantle, *Earth Planet. Sci. Lett.*, *39*, 349–357, doi:10.1016/0012-821X(78)90021-3.
- Mattinson, J. M. (1987), U-Pb ages of zircons: A basic examination of error propagation, *Chem. Geol.*, *66*, 151–162, doi:10.1016/0168-9622(87)90037-6.
- Mehl, L., B. R. Hacker, G. Hirth, and P. B. Kelemen (2003), Arc-parallel flow within the mantle wedge: Evidence from the accreted Talkeetna arc, south central Alaska, *J. Geophys. Res.*, *108*(B8), 2375, doi:10.1029/2002JB002233.
- Newberry, R. J., P. W. Layer, R. E. Burleigh, and D. N. Solie (1998), New $^{40}\text{Ar}/^{39}\text{Ar}$ dates for intrusion and mineral prospects in the eastern Yukon-Tanana Terrane, Alaska—Regional patterns and significance, in *Geologic Studies in Alaska*, edited by J. E. Gray and J. R. Riehe, *U.S. Geol. Surv. Prof. Pap.*, pp. 131–159.
- Onstott, T. C., V. B. Sisson, and D. L. Turner (1989), Initial argon in amphiboles from the Chugach Mountains, southern Alaska, *J. Geophys. Res.*, *94*, 4361–4372, doi:10.1029/JB094iB04p04361.
- Patchett, P. J., J. D. Vervoort, U. Söderlund, and V. J. Salters (2004), Lu-Hf and Sm-Nd isotopic systematics in chondrites and their constraints on the Lu-Hf properties of the Earth, *Earth Planet. Sci. Lett.*, *222*, 29–41, doi:10.1016/j.epsl.2004.02.030.
- Pavlis, T. L. (1983), Pre-Cretaceous crystalline rocks of the western Chugach Mountains, Alaska: Nature of the basement of the Jurassic Peninsular terrane, *Geol. Soc. Am. Bull.*, *94*, 1329–1344, doi:10.1130/0016-7606(1983)94<1329:PCROTW>2.0.CO;2.
- Pavlis, T. L., and S. M. Roeske (2007), The Border Ranges fault system, southern Alaska, in *Tectonic Growth of a Collisional Continental Margin: Crustal Evolution of Southern Alaska*, edited by K. D. Ridgway et al., *Geol. Soc. Am. Spec. Pap.*, *431*, pp. 95–127, doi:10.1130/2007.2431(05).
- Plafker, G., W. J. Nokleberg, and J. S. Lull (1989), Bedrock geology and tectonic evolution of the Wrangellia, Peninsular, and Chugach terranes along the Trans-Alaska Crustal Transect in the Chugach Mountains and southern Copper River basin, Alaska, *J. Geophys. Res.*, *94*, 4255–4295, doi:10.1029/JB094iB04p04255.
- Plafker, G., J. C. Moore, and G. R. Winkler (1994), Geology of the southern Alaska margin, in *The Geology of Alaska: Geology of North America*, edited by

- G. Plafker and H. G. Berg, pp. 389–450, *Geol. Soc. of Am.*, Boulder, Colorado.
- Reiners, P. W. (2005), Zircon (U-Th)/He thermochronometry, in *Thermochronology*, edited by P. W. Reiners and T. A. Ehlers, *Rev. Mineral. Geochem.*, 58, 151–176.
- Reiners, P. W., and M. T. Brandon (2006), Using thermochronology to understand orogenic erosion, *Annu. Rev. Earth Planet. Sci.*, 34, 419–466, doi:10.1146/annurev.earth.34.031405.125202.
- Reiners, P. W., T. L. Spell, S. Nicolescu, and K. A. Zanetti (2004), Zircon (U-Th)/He thermochronometry: He diffusion and comparisons with $^{40}\text{Ar}/^{39}\text{Ar}$ dating, *Geochim. Cosmochim. Acta*, 68, 1857–1887, doi:10.1016/j.gca.2003.10.021.
- Renne, P. R., R. Mundil, G. Balco, K. Min, and K. R. Ludwig (2010), Joint determination of ^{40}K decay constants and $^{40}\text{Ar}/^{40}\text{K}$ for the Fish Canyon sanidine standard, and improved accuracy for $^{40}\text{Ar}/^{39}\text{Ar}$ geochronology, *Geochim. Cosmochim. Acta*, 74, 5349–5367, doi:10.1016/j.gca.2010.06.017.
- Rioux, M., B. R. Hacker, J. Mattinson, P. Kelemen, J. Blusztajn, and G. E. Gehrels (2007), Magmatic development of an intra-oceanic arc: High-precision U-Pb zircon and whole-rock isotopic analyses from the accreted Talkeetna Arc, south-central Alaska, *Geol. Soc. Am. Bull.*, 119, 1168–1184, doi:10.1130/B25964.1.
- Rioux, M., J. Mattinson, B. Hacker, P. Kelemen, J. Blusztajn, K. Hanghøj, and G. Gehrels (2010), Intermediate to felsic middle crust in the accreted Talkeetna arc, the Alaska Peninsula and Kodiak Island, Alaska: An analogue for low-velocity middle crust in modern arcs, *Tectonics*, 29, TC3001, doi:10.1029/2009TC002541.
- Roeske, S. M., L. W. Snee, and T. L. Pavlis (2003), Dextral slip reactivation of an arc-forearc boundary during Late Cretaceous–Early Eocene oblique convergence in the northern Cordillera, in *Geology of a Transpressional Orogen Developed During Ridge-Trench Interaction Along the North Pacific Margin*, edited by V. B. Sisson, S. M. Roeske, and T. L. Pavlis, *Geol. Soc. Am. Spec. Pap.*, 371, 141–170.
- Scherer, E. E., K. L. Cameron, and J. Blichert-Toft (2000), Lu-Hf garnet geochronology: Closure temperature relative to the Sm-Nd system and the effects of trace mineral inclusions, *Geochim. Cosmochim. Acta*, 64, 3413–3432, doi:10.1016/S0016-7037(00)00440-3.
- Schoene, B., J. L. Crowley, D. J. Condon, M. D. Schmitz, and S. A. Bowring (2006), Reassessing the uranium decay constants for geochronology using ID-TIMS U-Pb data, *Geochim. Cosmochim. Acta*, 70, 426–445, doi:10.1016/j.gca.2005.09.007.
- Sisson, V. B., and T. C. Onstott (1986), Dating blueschist metamorphism: A combined $^{40}\text{Ar}/^{39}\text{Ar}$ and electron microprobe approach, *Geochim. Cosmochim. Acta*, 50, 2111–2117, doi:10.1016/0016-7037(86)90264-4.
- Söderlund, U., P. J. Patchett, J. D. Vervoort, and C. E. Isachsen (2004), The ^{176}Lu decay constant determined by Lu-Hf and U-Pb isotope systematics of Precambrian mafic intrusions, *Earth Planet. Sci. Lett.*, 219, 311–324, doi:10.1016/S0012-821X(04)00012-3.
- Stein, C. A., and S. Stein (1992), A model for the global variation in oceanic depth and heat flow with lithospheric age, *Nature*, 359, 123–129, doi:10.1038/359123a0.
- Trop, J. M., and K. D. Ridgeway (2007), Mesozoic and Cenozoic tectonic growth of southern Alaska: A sedimentary basin perspective, in *Tectonic Growth of a Collisional Continental Margin: Crustal Evolution of Southern Alaska*, edited by K. D. Ridgeway et al., *Geol. Soc. Am. Spec. Pap.*, 431, 55–94.
- Trop, J. M., D. A. Szuch, M. Rioux, and R. B. Blodgett (2005), Sedimentology and provenance of the Upper Jurassic Naknek Formation, Talkeetna Mountains, Alaska: Bearings on the accretionary tectonic history of the Wrangellia composite terrane, *Geol. Soc. Am. Bull.*, 117, 570–588, doi:10.1130/B25575.1.
- Van Orman, J. A., T. L. Grove, N. Shimizu, and G. D. Layne (2002), Rare earth element diffusion in a natural pyrope single crystal at 2.8 GPa, *Contrib. Mineral. Petrol.*, 142, 416–424, doi:10.1007/s004100100304.
- Wada, I., and K. Wang (2009), Common depth of slab-mantle decoupling: Reconciling diversity and uniformity of subduction zones, *Geochem. Geophys. Geosyst.*, 10, Q10009, doi:10.1029/2009GC002570.
- Winkler, G. R. (1992), Geologic map and summary geochronology of the Anchorage $1^\circ \times 3^\circ$ Quadrangle, southern Alaska, scale 1:250,000, *U.S. Geol. Surv. Misc. Invest. Ser. Rep.*, 1-2283.
- Winkler, G. R., M. L. Silberman, A. Grantz, R. J. Miller, and E. M. MacKevett Jr. (1981), Geologic map and summary geochronology of the Valdez quadrangle, southern Alaska, scale 1:250,000, *U.S. Geol. Surv. Open File Rep.*, 80-892-A.
- P. B. Gans and B. R. Hacker, Department of Earth Science, University of California, Santa Barbara, CA 93106, USA. (gans@geol.ucsb.edu; hacker@geol.ucsb.edu)
- P. B. Kelemen, Lamont-Doherty Earth Observatory, Earth Institute at Columbia University, P.O. Box 1000, Palisades, NY 10964, USA. (peterk@ldeo.columbia.edu)
- P. W. Layer, Department of Geology and Geophysics, University of Alaska, Fairbanks, Fairbanks, AK 99775, USA. (player@gi.alaska.edu)
- M. O. McWilliams, Earth Science and Resource Engineering, Commonwealth Scientific and Industrial Research Organisation, Pullenvale, Qld 4069, Australia. (mike.mcwilliams@csiro.au)
- P. W. Reiners, Department of Geosciences, University of Arizona, Tucson, AZ 85720, USA. (reiners@u.arizona.edu)
- M. Rioux, Department of Earth, Atmospheric, and Planetary Sciences, Massachusetts Institute of Technology, Cambridge, MA 02139, USA. (riouxm@mit.edu)
- U. Söderlund, Department of Earth and Ecosystem Sciences, Lund University, Sölvegatan 12, SE-223 62 Lund, Sweden. (ulf.soderlund@geol.lu.se)
- J. D. Vervoort, School of Earth and Environmental Sciences, Washington State University, Pullman, WA 99164, USA. (vervoort@wsu.edu)